Jpn. J. Infect. Dis., 66, 65-68, 2013

Short Communication

Composition of Hemagglutinin and Neuraminidase Affects the Antigen Yield of Influenza A(H1N1)pdm09 Candidate Vaccine Viruses

Masayuki Shirakura, Akira Kawaguchi, Masato Tashiro, and Eri Nobusawa*

Influenza Virus Research Center, National Institute of Infectious Diseases, Tokyo 208-0011, Japan

(Received August 8, 2012. Accepted October 24, 2012)

SUMMARY: To improve the hemagglutinin (HA) antigen yield of influenza A(H1N1)pdm09 candidate vaccine viruses, we generated 7:1, 6:2, and 5:3 genetic reassortant viruses between wild-type (H1N1)pdm09 (A/California/7/2009) (Cal7) and a high-yielding master virus, A/Puerto Rico/8/34 (PR8). These viruses contained the HA; HA and neuraminidase (NA); and HA, NA, and M genes, respectively, derived from Cal7, on a PR8 backbone. The influence of the amino acid residue at position 223 in Cal7 HA on virus growth and HA antigen yield differed between these reassortant viruses. NIIDRG-7, a 7:1 virus possessing arginine at position 223, exhibited a 10-fold higher 50% egg infectious dose (EID_{50}) (10.0 $\log_{10}EID_{50}$/ml) than the 5:3 and 6:2 viruses. It also had 1.5- to 3-fold higher protein (13.8 μg/ml of allantoic fluids) and HA antigen (4.1 μg/ml of allantoic fluids) yields than the 5:3 and 6:2 viruses, which possessed identical Cal7 HA proteins. However, the HA antigen yield of the other 7:1 virus, which possessed glutamine at position 223 was 60% of that of NIIDRG-7. In addition, a novel 6:2 virus possessing Cal7 HA and the NA of A/Wisconsin/10/98 (a triple reassortant swine-like H1N1 virus), produced 107% of the HA yield of NIIDRG-7. In this study, we showed that the balance between HA and NA in the influenza A(H1N1)pdm09 virus affects its protein and antigen yield.

In April 2009, a novel influenza A(H1N1)pdm09 virus was identified in the United States. Within 2 months, this virus had spread globally, causing the first pandemic of the 21st century (1). The A(H1N1)pdm09 virus is a novel reassortant virus that contains 6 gene segments from the North American triple-reassortant swine-influenza viruses. It also encompasses neuraminidase (NA) and M gene segments from the Eurasian swine influenza viruses (1,2). Due to the origin of the HA gene, the A(H1N1)pdm09 virus is antigenically different from the previous seasonal H1N1 viruses that circulated globally until April 2009 (3). To prevent the spread of the viruses through the population, the World Health Organization (WHO) Global Influenza Surveillance and Response System initiated the development of candidate vaccine viruses (CVVs) (4). Currently, influenza vaccine viruses are propagated in embryonated chicken eggs. However, human influenza isolates, in most cases, grow poorly in chicken eggs; and A(H1N1)pdm09 virus is not an exception. There have been efforts to develop high-growth reassortant viruses between A/California/7/2009 (Cal7) and a high-yielding master virus (A/Puerto Rico/8/34 [PR8] or its derivative) using the classical reassortment method (5,6) or by reverse genetics using plasmid DNAs (7-9). One such reassortant virus, X-179A, exhibited higher growth in eggs (hemagglutination [HA] titer, 2048) than the parental virus, Cal7 (HA titer, 64) (4). Despite the high HA titer of X-179A, the total protein and HA antigen yield was lower than that for the previous seasonal human H1N1 vaccine viruses (4). To overcome this disadvantage, we attempted to develop vaccine viruses with higher growth in eggs and higher protein yield. We used 12 plasmid-based reverse genetics system and the high-growth PR8 virus (UW strain) as the backbone virus (Table 1) (8). For pandemic vaccine viruses, the WHO recommends that the reassortant virus possesses at least the HA and NA genes of the pandemic virus with the remaining genes originating from PR8 (6:2) (10). However, an improvement in virus growth or antigen yield, relative to 6:2 viruses, was observed with H5N1 reassortant viruses possessing the HA (7:1), HA/NA/PB1 (5:3), or HA/NA/M (5:3) from H5 viruses (11). In addition, studies have shown that there are different residues (D/Q, G/Q, or D/R) at the receptor-binding site of Cal7 HA at positions 222/223 (H1HA numbering) (4,12). The residues at these positions reportedly affect the receptor binding specificity of H1N1, H2N2, and H3N2 influenza viruses (13-17). In this study, we examined the effect of gene constellations and amino acid residues at 222/223 in Cal7 HA on virus growth and antigen yield.

We first developed three 6:2 reassortant viruses with D/Q, G/Q, and D/R at positions 222/223 using the appropriate cloned Cal7 HA cDNAs (Table 1). The HA titer of the virus with G/Q was 64. Passaging the viruses 4 times in embryonated chicken eggs did not improve the HA titer. However, the HA titers of the D/Q and D/R viruses increased to 128 and 512, respectively (Table 1). Next, to assess the impact of D/Q and D/R at positions 222/223 and the impact of the gene constellations on virus growth and infectivity, we develped 5:3 (NIIDRG-3, -6) and 7:1 (NIIDRG-7, -8) reassortant viruses, in addition to the 6:2 viruses (NIIDRG-1, -5) (Table 1). We performed 50% egg infective dose (EID_{50}) assays and found that infectivity increased

*Corresponding author: Mailing address: Influenza Virus Research Center, National Institute of Infectious Diseases, Gakuen 4-7-1, Musashi-Murayamashi, Tokyo 208-0011, Japan. Tel: +81-42-848-7168, Fax: +81-42-561-6124, E-mail: nobusawa@nih.go.jp

Table 1. Differences in the amino acid sequences of HA and the infectivity titers of viruses

Virus[1)]	Passage history	Gene constellation	Amino acid at the indicated HA positions[2)]					EID_{50} (log_{10}/EID_{50} ml)[3)]	
			125	191	209	222	223	Exp. 1	Exp. 2
A/California/7/2009	—	—	N	L	K	D/G	Q/R	n.d.	n.d.
X-179A	E7/E1/E6	5:3	·	·	T	D	R	9.4	9.3
NIIDRG-1	LLC1E2	6:2	·	I	·	D	Q	8.3	8.4
NIIDRG-3	LLC1E2	5:3	·	I	·	D	Q	8.2	8.3
NIIDRG-5	LLC1E4	6:2	·	·	·	D	R	9.1	9.0
NIIDRG-6	LLC1E5	5:3	N/D	·	·	D	R	9.0	8.9
NIIDRG-7	LLC1E2	7:1	·	·	·	D	R	9.9	10.0
NIIDRG-8	LLC1E3	7:1	·	I	·	D	Q	9.3	9.1

1): Reassortant viruses were generated by co-transfecting 12 plasmid DNAs into qualified LLCMK2 cells using FuGENE HD Transfection Reagent (Roche) (LLC1) (8). Approximately 18 h post-transfections, the cells were washed, and the medium was replaced with Opti-Pro SFM medium (Invitrogen) containing 1 μg/ml of TrypZean (SIGMA). The supernatant was harvested at 48 h post-transfection and used to inoculate 10-day-old specific-pathogen-free (SPF) embryonated chicken eggs to amplify the rescued viruses. For each reassortant virus, the genetic sequences of HA and/or NA and/or M derived from Cal7 were verified by sequencing the RT-PCR products amplified from viral RNA. All the manipulations were performed in accordance with the Good Manufacturing Practice of NIID.

2): H1 numbering; all changes relative to A/California/7/2009.

3): The EID_{50} was determined as follows: each virus was serially diluted from 10^{-5} to 10^{-11}. Six 10 to 11 day-old embryonated chicken eggs were infected with 0.2 ml of virus for each dilution. An aliquot of the allantoic fluid was harvested from each of the eggs at 48 h post-infection. An HA assay was performed for each allantoic fluid, using 0.5% turkey erythrocytes. The EID_{50} was calculated by using the formula of Reed and Muench. The results are from two separate experiments.

n.d., not done.

among the reassortant viruses (in the order 5:3, 6:2, and 7:1) possessing the identical amino acid residues at positions 222/223. In addition, the influence of 223R on the EID_{50} was greater than that of 223Q, as determined by evaluating viruses with the same gene constellations (Table 1). The HA titers and EID_{50} values were nearly parallel for each virus. Among the reassortant viruses, NIIDRG-7 exhibited the highest growth (HA titer, 1024) and EID_{50} (Table 1). Residue 223 is located on the 220-loop of the receptor-binding site of HA. Avian H1HA has close contact between 223Q and the Gal-2 of α2-3 linked sialylated glycans. However, similar contacts between the A(H1N1)pdm09 HA of A/California/4/2009 and α2-3 linked sialylated glycans are absent (18). The presence of 223R instead of 223Q might overcome the unfavorable interactions between Cal7 HA and α2-3 linked sialylated glycans, which are prevalent in the chorioallantois of chicken eggs. In the case of 223Q viruses (NIIDRG-1, -3, and -8), all rescued viruses possessed an additional substitution, i.e., L191I. The L191I substitution might facilitate viral rescue and amplification in eggs, as was observed with other reassortant viruses derived from A/California/4/2009 (12). However, this substitution did not have a stronger influence on virus growth than that observed with 223R.

The total protein yield (TPY) of the purified NIIDRG-1, -3, and -5 to -8 and X-179A viruses was determined by using the bicinchoninic acid (BCA) protein assay (Pierce, Rockford, Ill., USA), according to the manufacturer instructions (Fig. 1). Among the viruses subjected to the assay, NIIDRG-7 exhibited the highest TPY (13.8 μg/ml allantoic fluid [AF]), whereas X-179A had a TPY of 10.4 μg/ml AF. The other viruses exhibited TPYs similar to or lower than that of X-179A (Fig. 1). A correlation between virus proliferation and TPY was observed primarily with the resultant viruses.

The HA yield of each virus was calculated using the TPY and the results of the SDS-PAGE analysis (Fig. 1). The HA content relative to the total protein content of

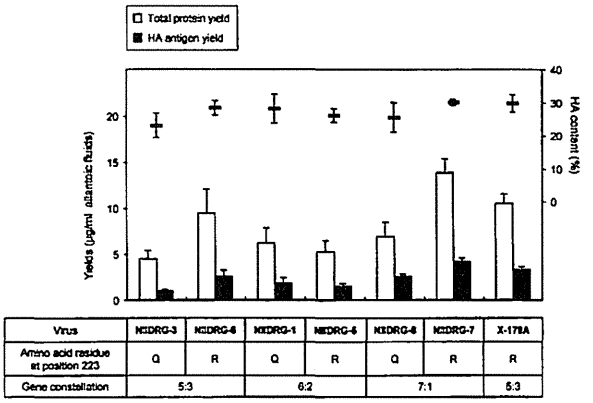

Fig. 1. Average yield (μg) of total protein, HA antigen per ml of allantoic fluids and the average HA content (%) of each virus concentrate. Ten-day-old embryonated chicken eggs were inoculated with NIIDRG-1, -3, and -5 to -8 viruses. Forty-eight hours post infection, the allantoic fluid was collected. The viruses were purified by ultracentrifugation using 20% sucrose at 35,000 rpm for 60 min at 4°C. The pellet was re-suspended in a small volume of buffer, which was used as the purified concentrate. The method for preparation of the virus concentrate differed from the method used by others (4,21); therefore, we re-assessed the total protein yield of X-179A and NIIDRG-7. We used viruses concentrated by methods similar to those used by others (4,21), that is, viruses were grown in 50 eggs and purified using 10–40% continuous sucrose gradient with centrifugation at 35,000 rpm for 35 min at 4°C. The total protein yield of X-179A and NIIDRG-7 was estimated at 4.5 mg/50 eggs and 6.25 mg/50 eggs, respectively. The HA content was calculated using the results from the SDS-PAGE analysis, which are shown in Figure 2. The SDS-PAGE results were captured and analyzed using a CS analyzer (ATTO), and the ratio of HA protein to total proteins was calculated. The total HA yields were calculated from the total protein yields and the relative HA contents. Each value is the average of values from 3 analyses.

NIIDRG viruses ranged between 23% (NIIDRG-3) and 30% (NIIDRG-7). NIIDRG-7 had the highest HA yield (4.1 μg/ml AF) whereas X-179A had an HA yield of 3.3

μg/ml AF (Fig. 1). NIIDRG-6 and -8 also exhibited low HA yield (2.5 μg/ml AF). The remaining viruses had yields much lower than that of NIIDRG-7.

The functional balance between HA and NA is known to affect the virus growth (19,20). The novel gene constellation of the A(H1N1)pdm09 virus may not result in the optimal balance between HA and NA activity. The difference in TPY between NIIDRG-5 and NIIDRG-7 is attributable to the imbalance in HA and NA activity. Cal7 HA is genetically close to HA in the triple-reassortant swine-like H1N1 virus, A/Wisconsin/10/98 (Wis98) (3). The similarity of HA1 is 93% between Cal7 and Wis98. To improve the compatibility of HA and NA, we developed another 6:2 reassortant virus, Cal7/Wis98 which harbored Cal7 HA and Wis98 NA with a PR8 backbone. The HA yield (4.4 μg/ml AF) and the TPY (15.2 μg/ml AF) were slightly higher than that of NIIDRG-7. This suggests that the low TPY and HA yield of NIIDRG-5 was a result of the poor compatibility of HA and NA of Cal7.

During the preparation of this manuscript, Harvey et al. reported a new CVV (6:2) with a chimeric sequence derived from PR8 and Cal7 HA (NIBRG-119). This new CVV exhibited improved growth as compared to the current vaccine virus (6:2) (NIBRG-121) (21). Based on their results, we created a new 7:1 reassortant virus by exchanging the 3′- and 5′-non-coding region domains, signal peptide, transmembrane (TM) domain, and cytoplasmic tail of Cal7 HA with those of PR8 (NIIDRG-7.1) (Fig. 2A). NIIDRG-7.1 exhibited an improved HA content (40.1 ± 1.23%) (Fig. 2B) and HA yield (5.2 μg/ml AF). However, it still had a TPY (13.1 μg/ml AF) similar to that of NIIDRG-7. Our result proved the hypothesis proposed by Harvey et al.; they stated that the TM domain of PR8HA plays a role in the efficient incorporation of HA into viral particles, which is caused by the increased association of HA with glycosphingolipid-enriched, detergent-resistant plasma membrane domains. In the case of NIBRG-119, the TPY was higher, but not the HA yield. Although both viruses showed similar HA yields, the mechanisms responsible for improvement might be different.

We performed hemagglutination inhibition (HAI) assays using ferret antisera against the reassortant viruses in order to determine their antigenic characteristics (Table 2). All NIIDRG viruses were antigenically similar to wild-type A(H1N1)pdm09, Cal7, and A/Narita/1/2009, and the vaccine virus X-179A. However, the NIIDRG viruses were distinct from A/Brisbane/59/2007, a past seasonal H1N1 virus (Table 2).

To improve the protein/antigen yields of A(H1N1)pdm09 CVVs, genetic alterations have been introduced into the packaging signal and the oligosaccharide moiety of Cal7 HA (21,22). In this study, we showed that the composition of HA and NA must be controlled to achieve a high protein yield. Although NA immunogenicity of the original pandemic virus is significant, if the antigen yield is extremely low, as observed for the A(H1N1)pdm09 CVV, we can also con-

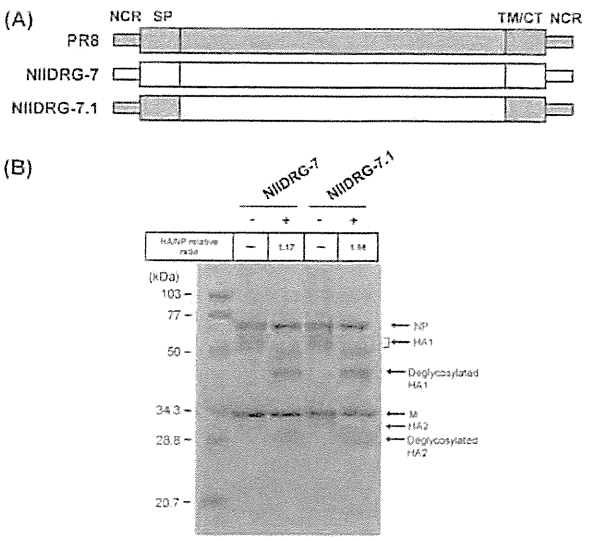

Fig. 2. (A) Schematic diagram of the HA chimera. Domains derived from Cal7 and PR8 are shown in white and black, respectively. NCR, non-coding region; SP, signal peptide; TM/CT, transmembrane and cytoplasmic tail domains of the HA. (B) SDS-PAGE analysis of NIIDRG-7 and NIIDRG-7.1. The purified viruses (6 μg) were treated with (+) or without (−) 10 units of PNGase F according to the manufacturer's instructions (New England Biolabs). Samples were incubated in a total volume of 20 μl at 37°C overnight, and the reducing agent was added before the samples were loaded on 10% SDS-PAGE gels. The relative ratio of HA to NP is shown as the average of the values.

Table 2. Antigenic analysis of viruses

Virus	Titer[1] of ferret antiserum against indicated virus:			
	A/Brisbane/59/2007	A/California/7/2009	A/Narita/1/2009	NYMC X-179A
A/Brisbane/59/2007	**640**	<10	<10	<10
A/California/7/2009	<10	**2560**	10240	2560
A/Narita/1/2009	<10	2560	**10240**	5120
NYMC X-179A	<10	5120	10240	**5120**
NIIDRG-1	<10	2560	5120	1280
NIIDRG-3	<10	1280	5120	1280
NIIDRG-5	<10	1280	5120	1280
NIIDRG-6	<10	1280	5120	1280
NIIDRG-7	<10	2560	5120	2560
NIIDRG-8	<10	1280	5120	1280

[1]: HAI assay was performed with 0.5% turkey erythrocytes. HAI titers are presented as the reciprocal value of the highest serum dilution which inhibited hemagglutination ability of the viruses. The homologous titers are boldfaced.

sider the development of a CVV with a different gene constellation without genetic alterations.

Acknowledgments We thank the members of the Influenza Virus Research Center of NIID for their great contributions to the A(H1N1)pdm09 vaccine development project. We thank Hideki Hasegawa and Takato Odagiri for providing the ferret antisera against A/California/7/2009, A/Narita/1/2009, and NYMC X-179A; the Centers for Disease Control and Prevention for providing A/California/7/2009 and ferret antisera against A/Brisbane/59/2007; Doris Bucher at New York Medical College for providing NYMC X-179A; The Chemo-Sero-Therapeutic Research Institute, Japan for their quality control of the LLCMK2 cells; and Yoshi Kawaoka for providing the plasmid DNA for the reverse genetics technique.

This work was supported by funding from the Ministry of Health, Labour and Welfare of Japan.

Conflict of interest None to declare.

REFERENCES

1. Dawood, F.S., Jain, S., Finelli, L., et al. (2009): Emergence of a novel swine-origin influenza A (H1N1) virus in humans. N. Engl. J. Med., 360, 2605–2615.
2. Maldonado, J., Van Reeth, K., Riera, P., et al. (2006): Evidence of the concurrent circulation of H1N2, H1N1 and H3N2 influenza A viruses in densely populated pig areas in Spain. Vet. J., 172, 377–381.
3. Garten, R.J., Davis, C.T., Russell, C.A., et al. (2009): Antigenic and genetic characteristics of swine-origin 2009 A(H1N1) influenza viruses circulating in humans. Science, 325, 197–201.
4. Robertson, J.S., Nicolson, C., Harvey, R., et al. (2011): The development of vaccine viruses against pandemic A(H1N1) influenza. Vaccine, 29, 1836–1843.
5. Kilbourne, E.D. (1969): Future influenza vaccines and the use of genetic recombinants. Bull. World Health Organ., 41, 643–645.
6. Kilbourne, E.D., Schulman, J.L., Schild, G.C., et al. (1971): Related studies of a recombinant influenza-virus vaccine. I. Derivation and characterization of virus and vaccine. J. Infect. Dis., 124, 449–462.
7. Fodor, E., Devenish, L., Engelhardt, O.G., et al. (1999): Rescue of influenza A virus from recombinant DNA. J. Virol., 73, 9679–9682.
8. Neumann, G., Watanabe, T., Ito, H., et al. (1999): Generation of influenza A viruses entirely from cloned cDNAs. Proc. Natl. Acad. Sci. USA, 96, 9345–9350.
9. Hoffmann, E., Neumann, G., Kawaoka, Y., et al. (2000): A DNA transfection system for generation of influenza A virus from eight plasmids. Proc. Natl. Acad. Sci. USA, 97, 6108–6113.
10. Wood, J.M. and Robertson, J.S. (2004): From lethal virus to life-saving vaccine: developing inactivated vaccines for pandemic influenza. Nat. Rev. Microbiol., 2, 842–847.
11. Rudneva, I.A., Timofeeva, T.A., Shilov, A.A., et al. (2007): Effect of gene constellation and postreassortment amino acid change on the phenotypic features of H5 influenza virus reassortants. Arch. Virol., 152, 1139–1145.
12. Chen, Z., Wang, W., Zhou, H., et al. (2010): Generation of live attenuated novel influenza virus A/California/7/09 (H1N1) vaccines with high yield in embryonated chicken eggs. J. Virol., 84, 44–51.
13. Matrosovich, M., Tuzikov, A., Bovin, N., et al. (2000): Early alterations of the receptor-binding properties of H1, H2, and H3 avian influenza virus hemagglutinins after their introduction into mammals. J. Virol., 74, 8502–8512.
14. Liu, J., Stevens, D.J., Haire, L.F., et al. (2009): Structures of receptor complexes formed by hemagglutinins from the Asian influenza pandemic of 1957. Proc. Natl. Acad. Sci. USA, 106, 17175–17180.
15. Rogers, G.N., Paulson, J.C., Daniels, R.S., et al. (1983): Single amino acid substitutions in influenza haemagglutinin change receptor binding specificity. Nature, 304, 76–78.
16. Stevens, J., Blixt, O., Glaser, L., et al. (2006): Glycan microarray analysis of the hemagglutinins from modern and pandemic influenza viruses reveals different receptor specificities. J. Mol. Biol., 355, 1143–1155.
17. Xu, R., Mcbride, R., Paulson, J.C., et al. (2010): Structure, receptor binding, and antigenicity of influenza virus hemagglutinins from the 1957 H2N2 pandemic. J. Virol., 84, 1715–1721.
18. Xu, R., Mcbride, R., Nycholat, C.M., et al. (2012): Structural characterization of the hemagglutinin receptor specificity from the 2009 H1N1 influenza pandemic. J. Virol., 86, 982–990.
19. Lu, B., Zhou, H., Ye, D., et al. (2005): Improvement of influenza A/Fujian/411/02 (H3N2) virus growth in embryonated chicken eggs by balancing the hemagglutinin and neuraminidase activities, using reverse genetics. J. Virol., 79, 6763–6771.
20. Octaviani, C.P., Li, C., Noda, T., et al. (2011): Reassortment between seasonal and swine-origin H1N1 influenza viruses generates viruses with enhanced growth capability in cell culture. Virus Res., 156, 147–150.
21. Harvey, R., Guilfoyle, K.A., Roseby, S., et al. (2011): Improved antigen yield in pandemic H1N1 (2009) candidate vaccine viruses with chimeric hemagglutinin molecules. J. Virol., 85, 6086–6090.
22. Nicolson, C., Harvey, R., Johnson, R., et al. (2012): An additional oligosaccharide moiety in the HA of a pandemic influenza H1N1 candidate vaccine virus confers increased antigen yield in eggs. Vaccine, 30, 745–751.

frontiers in MICROBIOLOGY

ORIGINAL RESEARCH ARTICLE
published: 18 December 2013
doi: 10.3389/fmicb.2013.00398

The N-terminal region of influenza virus polymerase PB1 adjacent to the PA binding site is involved in replication but not transcription of the viral genome

Nguyen Trong Binh, Chitose Wakai, Atsushi Kawaguchi and Kyosuke Nagata*

Department of Infection Biology, Faculty of Medicine and Graduate School of Comprehensive Human Sciences, University of Tsukuba, Tsukuba, Japan

Edited by:
Abraham L. Brass, University of Massachusetts Medical School, USA

Reviewed by:
Fumitaka Momose, Kitasato University, Japan
Natalia A. Ilyushina, U.S. Food and Drug Administration, USA
Takashi Kuzuhara, Tokushima Bunri University, Japan

***Correspondence:**
Kyosuke Nagata, Department of Infection Biology, Faculty of Medicine and Graduate School of Comprehensive Human Sciences, University of Tsukuba, 1-1-1 Tennodai, Tsukuba 305-8575, Japan
e-mail: knagata@md.tsukuba.ac.jp

The influenza virus genome forms viral ribonucleoprotein (vRNP) complexes with nucleoprotein and viral RNA-dependent RNA polymerases (RdRp), PB1, PB2, and PA subunits. The vRNP complex catalyzes both genome replication and transcription reactions. PB1 contains the motifs highly conserved among RdRps and functions as a catalytic subunit of RdRp. The N-terminal region of PB1 between amino acid (a.a.) positions 1–83 contains both putative vRNA and cRNA promoter binding sites and a PA binding site. However, except for the PA binding site, the crystal structure and the function of the N-terminal region of PB1 are poorly understood. Here, we have examined the functional structure of the N-terminal region of PB1. The regions between a.a. positions 1–50 are highly conserved between influenza A and B viruses, but amino acids at positions 16, 27, and 44 are different between two viruses. To elucidate the functional importance of these amino acids in replication and transcription of the viral genome, we generated viruses containing mutations at these positions by reverse genetics and examined replication and transcription activities of these mutants. We found that a.a. positions 27 and 44 are responsible for the viral replication activity but not transcription activity.

Keywords: influenza virus, promoter binding, replication, reverse-genetics, RNA-dependent RNA polymerase, transcription

INTRODUCTION

Influenza A and B viruses contain eight-segmented and negative-stranded RNAs (vRNA) as its genome. Each segment is encapsidated by nucleoprotein (NP) and associated with viral RNA-dependent RNA polymerases (RdRp) to form viral ribonucleoprotein (vRNP) complexes. The vRNP complex is a basic unit for both genome replication and transcription (Nagata et al., 2008).

The viral RdRp is a heterotrimer consisting of PB1, PB2, and PA subunits. Among them, PB1 functions as a catalytic subunit and assembly core of RdRp (Biswas and Nayak, 1996; Gonzalez et al., 1996; Toyoda et al., 1996; Zurcher et al., 1996; Ohtsu et al., 2002). The crystal structure of the interaction domains between N-terminal region of PB1 and C-terminal region of PA, and between C-terminal region of PB1 and N-terminal region of PB2 were resolved (He et al., 2008; Obayashi et al., 2008). PB1 contains the motifs highly conserved among RdRps, putative nucleotide-binding sites, and vRNA and cRNA promoter binding sites (Asano and Ishihama, 1997; Li et al., 1998; Gonzalez and Ortin, 1999a,b; Kolpashchikov et al., 2004) (**Figure 1A**).

The N-terminal region of PB1 (1–83 a.a.) contains both putative vRNA and cRNA promoter binding sites. However, except for the PA binding site (1–15 a.a.), the function of this region was poorly understood. Alignment of amino acid sequences revealved that the a.a. positions 1–50 was highly conserved between influenza A and B viruses except for the amino acid positions 16, 27, and 44. To identify the functional importance of these positions for the viral RNA synthesis, we determined the replicational and transcriptional activities using mutant viruses. Our results strongly suggest that the a.a. positions 27 and 44 are involved in replication process but not transcription process.

MATERIALS AND METHODS

BIOLOGICAL MATERIALS

Monolayer cultures of 293T and MDCK cells were maintained at 37°C with 5% CO_2 in Dulbecco's Modified Eagle Medium (DMEM) and minimal essential medium (MEM) (Nissui), respectively, supplemented with 10% fetal bovine serum (Bovogen). Influenza virus strain A/WSN/33 (WSN) was prepared as previously described (Kawaguchi et al., 2005). Cycloheximide (CHX) was purchased from Sigma-Aldrich.

GENERATION OF RECOMBINANT VIRUSES

To construct plasmids from which human DNA-dependent RNA polymerase I (Pol I) transcribes mutated vRNAs, we amplified fragments containing mutated segment 2 by PCR using a plasmid containing wild type WSN segments in pHH21 vector (Neumann et al., 1999) as a template with sets of phosphorylated primers (see Table S1 in the supplemental material). The amplified PCR products were self-ligated followed by sequencing. To generate recombinant viruses containing viral RNAs of WSN and mutated segment 2, reverse genetics system was used as described previously (Neumann et al., 1999). After 48 h post transfection (hpt), aliquots of cell culture supernatants were used for virus

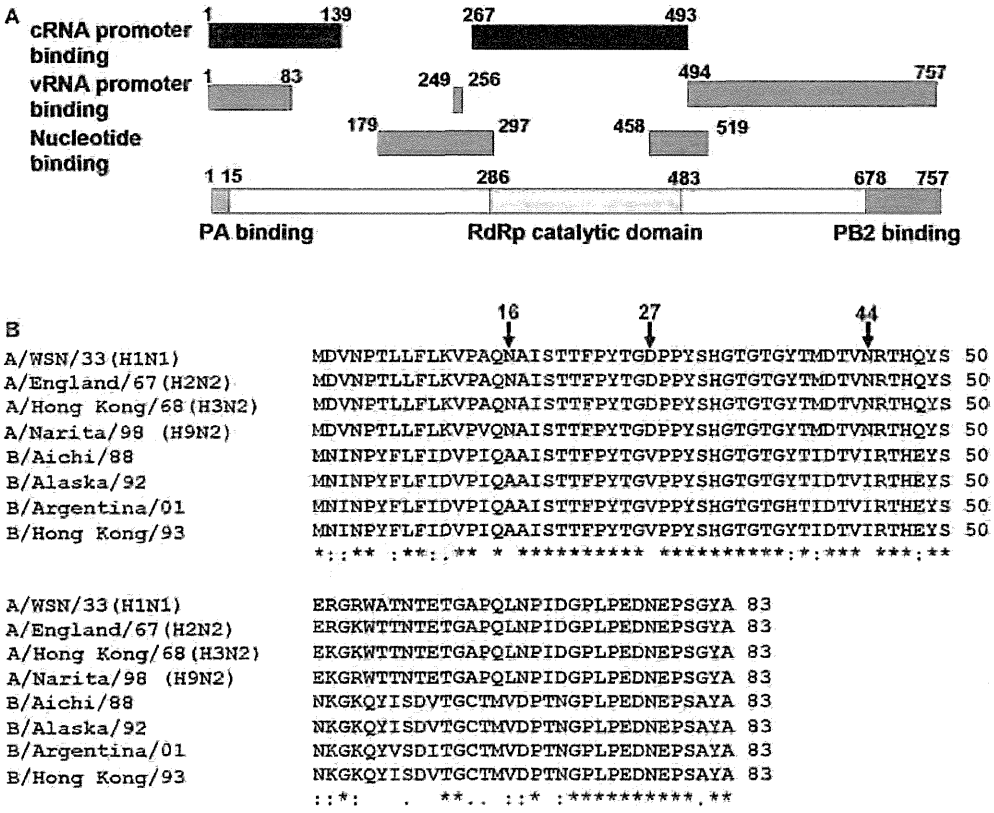

FIGURE 1 | Structure of PB1 subunit. (A) A diagrammatic representation of PB1. Black bar, cRNA promoter binding sites; gray bar, vRNA promoter binding sites; black and white vertical stripes, nucleotide binding sites; black and white horizontal stripes, PB2 binding site; black waved lines, PA binding site, and black dots, RNA dependent-RNA polymerase catalytic domain. **(B)** Alignment of amino acid sequences of putative RNA binding region common to vRNA and cRNA promoters (1–83 a.a.) among influenza A and influenza B viruses. PB1 sequences of A/WSN/33, A/WSN/1933 (H1N1); A/England/67, A/England/10/67 (H2N2); A/Hong Kong/68, A/Hong Kong/1/1968 (H3N2); A/Narita/98, A/parakeet/Narita/92A/98 (H9N2). These strains are picked up from different clades and periods of PB1 gene phylogenetic tree (Taubenberger et al., 2005); B/Aichi/88, B/Aichi/5/88; B/Alaska/92, B/Alaska/03/1992; B/Argentina/01, B/Argentina/132/2001; and B/Hong Kong/93, B/Hong Kong/02/1993. Sequences were aligned with CLUSTAL W. Asterisk (*), identical residues; colon (:), conserved residues, and dot (.), semi-conserved residues.

amplification in MDCK cells. At 48 h post infection (hpi), the culture fluid was collected, and the virus titer of these recombinant viruses was determined by plaque assays.

RNA ANALYSIS BY qRT-PCR

MDCK cells were infected with recombinant viruses at the multiplicity of infection (MOI) of 2.5. At 9 hpi, total RNA was isolated by the acid guanidine-phenol-chloroform method. To measure the accumulation levels of viral mRNA, cRNA, and vRNA, quantitative RT-PCR (qRT-PCR) was performed. Total RNAs were subjected to reverse transcription using ReverTraAce (Toyobo) with either (i) oligo $(dT)_{20}$, (ii) 5′-AGTAGAAACAAGGGTATTTTTCTTTA-3′, or (iii) 5′-GACGATGCAACGGCTGGTCTG-3′ for synthesizing cDNA from segment 5 mRNA, cRNA, and vRNA, respectively (Kawaguchi and Nagata, 2007; Sugiyama et al., 2009). The synthesized single-stranded cDNAs were subjected to real-time quantitative PCR analysis (Thermal Cycler Dice real-time system TP800; TaKaRa) with SYBR Premix Ex *Taq* (TaKaRa) and a set of specific primers for segment 5 cDNA (see supplementary methods). The levels of these RNAs were normalized by the amount of cellular β-actin mRNA measured using specific primers (see supplementary methods). These results are averages from three independent experiments with standard deviations. The level of significance was determined by Student's *t*-test (unpaired).

RESULTS

RNA SYNTHESIS OF INFLUENZA A MUTANT VIRUSES CONTAINING INFLUENZA B VIRUS-TYPE AMINO ACID SIGNATURES

The N-terminal region of PB1 (1–83 a.a.) contains the PA binding site and both putative vRNA and cRNA promoter binding sites (**Figure 1A**). It is shown by alignment of amino acid sequences that the PB1 region between a.a. positions 1–50 are highly conserved between influenza A and B viruses, while the region between a.a. positions 51–83 differ between two viruses (**Figure 1B**). In the highly conserved region, except for the PA binding site, a.a. at positions 16, 27, and 44 are different between these viruses. Furthermore, these a.a. positions in PB1 are conserved more than 99% of influenza A and B viruses deposited in the NCBI Influenza Virus Sequence Database (**Table 1**). To elucidate the functional importance of these a.a. for viral RNA

Table 1 | Conservation of amino acid position 16, 27, and 44 in PB1.

Virus type	a.a. position	Mutation	No. of strains (total strains)	Percentage
INFLUENZA A VIRUS				
	16	N (wild type)	7228 (7259)	99.6%
		S	24 (7259)	0.3%
		D	4 (7259)	0.1%
		K	1 (7259)	0.0%
		H	1 (7259)	0.0%
		Y	1 (7259)	0.0%
	27	D (wild type)	7250 (7259)	99.9%
		N	4 (7259)	0.1%
		E	3 (7259)	0.0%
		G	2 (7259)	0.0%
	44	N (wild type)	7204 (7259)	99.2%
		S	42 (7259)	0.6%
		T	11 (7259)	0.2%
		D	2 (7259)	0.0%
INFLUENZA B VIRUS				
	16	A (wild type)	1412 (1412)	100%
	27	V (wild type)	1412 (1412)	100%
	44	I (wild type)	1409 (1412)	99.8%
		V	3 (1412)	0.2%

The conservation of amino acid position 16, 27, and 44 in PB1 was calculated by using 7259 sequences of human and avian influenza A strains and 1412 sequences of influenza B strains listed at the NCBI Influenza Sequence Database.

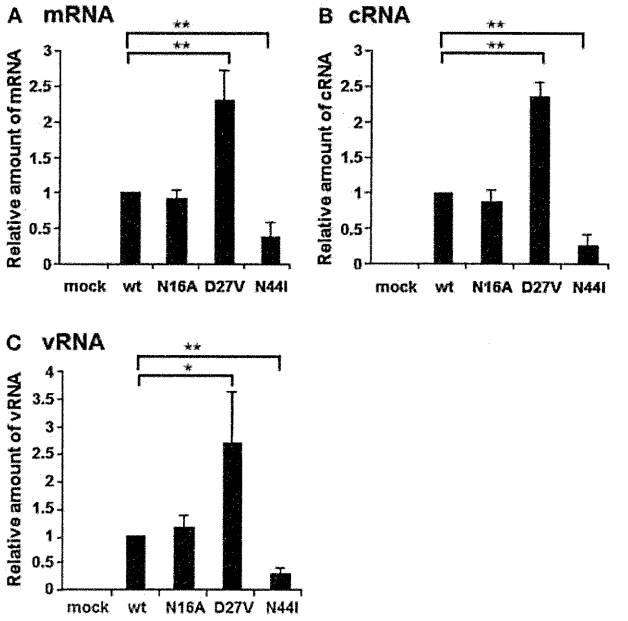

FIGURE 2 | Comparison of RNA synthesis of mutant influenza A viruses containing amino acids specific for influenza B viruses. The amino acids, N, D, and N at the positions 16, 27, and 44 were mutated to A, V, and I, respectively. MDCK cells were infected with mutant viruses at MOI of 2.5. At 9 hpi, the accumulation levels of viral mRNA **(A)**, cRNA **(B)**, and vRNA **(C)** were measured by qRT-PCR, and the amounts of these RNAs were normalized by that of cellular actin mRNA. These results are averages from three independent experiments with standard deviations. $*p < 0.05$; $**p < 0.01$.

synthesis, we generated influenza A viruses containing Ala at the a.a. position 16 (N16A), Val at the a.a. position 27 (D27V), and Ile at the a.a. position 44 (N44I) by reverse genetics. We examined the RdRp activity by measuring the accumulation levels of viral mRNA, cRNA, and vRNA by qRT-PCR (**Figure 2**). The levels of all three type RNAs from D27V were increased compared with those from wild type and N16A virus, while those from N44I were significantly decreased. Based on the result that mutations at the positions 27 and 44 affect the synthesis activity of all viral RNAs equally, there could be two possibilities: (i) these mutations affect on the vRNA promoter recognition and followed by cRNA/mRNA synthesis, but do not affect on the cRNA promoter recognition and followed by vRNA synthesis, or (ii) these mutations affect independently the synthesis of each viral RNA, but total effects leads similar outputs in the synthesis of all viral RNAs.

To elucidate whether these mutations affect genome replication (cRNA and vRNA synthesis) and/or transcription (viral mRNA synthesis) activities, we measured the primary transcription activity using cycloheximide (CHX), a potent inhibitor of protein synthesis (**Figure 3**). It is shown that CHX suppresses viral protein synthesis and thereby leads to degradation of replicated virus genome RNA but not viral mRNA since newly vRNP formation was repressed (Vreede et al., 2004; Kawaguchi et al., 2005). We utilized this method to measure the primary transcription activity that depends just only on incoming vRNP and is not affected by the replication process. In the presence of CHX, the levels of viral mRNA and vRNA were measured by qRT-PCR, and the transcription activity was represented as a ratio of viral mRNA/vRNA. This result shows that the transcription activity is not affected by these mutations, and thereby strongly suggests that these mutations affect the replication activity.

AMINO ACID PROPERTIES AT a.a. POSITIONS 27 AND 44 FOR THE RNA SYNTHESIS ACTIVITY

Aspartate at the position 27 is highly conserved among influenza A viruses, except for an H4N8 strain isolated from least sandpiper that contains asparagine (GenBank: ACI90144.1). We generated D27E and D27N in addition to D27V (**Figure 4**). The RNA levels of mRNA, cRNA, and vRNA of D27N and D27V were increased significantly compared with those of wild-type and D27E. One of possible interpretations is that uncharged amino acids at a.a. position 27 may enhance the RNA synthesis.

The mutation at the a.a. position 44 reduced the replication activity (**Figure 2**). To clarify the importance of the a.a. at this position, we additionally generated N44D and N44Q viruses in addition to N44I and examined the RNA synthesis activity (**Figure 5**). The synthesis level of each viral RNA of N44I was decreased largely, while the amounts of mRNA and cRNA of N44D and N44Q were similar to those of wild type. In addition, the amount of vRNA of N44Q was more than that of wild type.

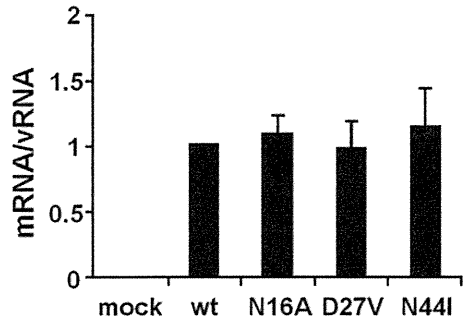

FIGURE 3 | Primary transcription activity of mutant influenza A viruses containing amino acids specific to influenza B viruses. MDCK cells were infected with mutant viruses at MOI of 2.5 and incubated in the presence of 1.0 μg/ml of CHX. At 9 hpi, the accumulation levels of viral mRNA and vRNA were measured by qRT-PCR, and the amounts of these RNAs were normalized by that of cellular actin mRNA. The transcription activity is represented as a ratio of the amount of viral mRNA to that of vRNA. These results are averages from three independent experiments with standard deviations.

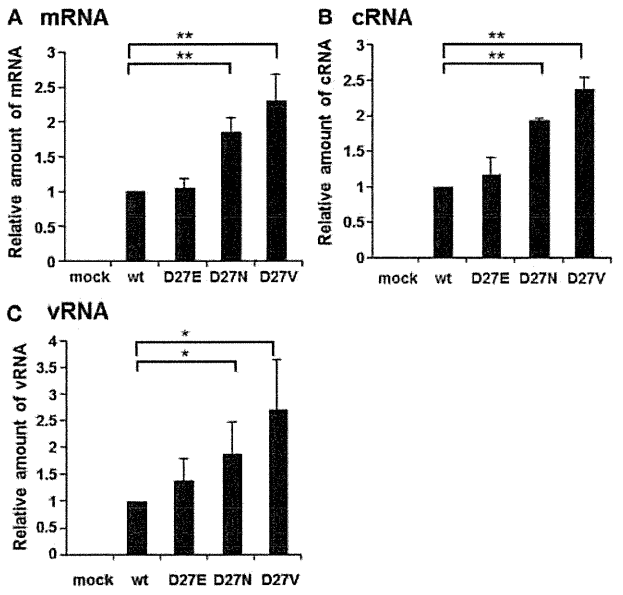

FIGURE 4 | RNA synthesis of viruses containing mutations at the amino acid position 27. Wild-type virus and mutant viruses containing amino acids D and E, N, and V, respectively, at the a.a. position 27 were infected into MDCK cells at MOI of 2.5. At 9 hpi, the accumulation levels of viral mRNA **(A)**, cRNA **(B)**, and vRNA **(C)** were measured by qRT-PCR, and the amounts of these RNAs were normalized by that of cellular actin mRNA. These results are averages from three independent experiments with standard deviations. $^{*}p < 0.05$; $^{**}p < 0.01$.

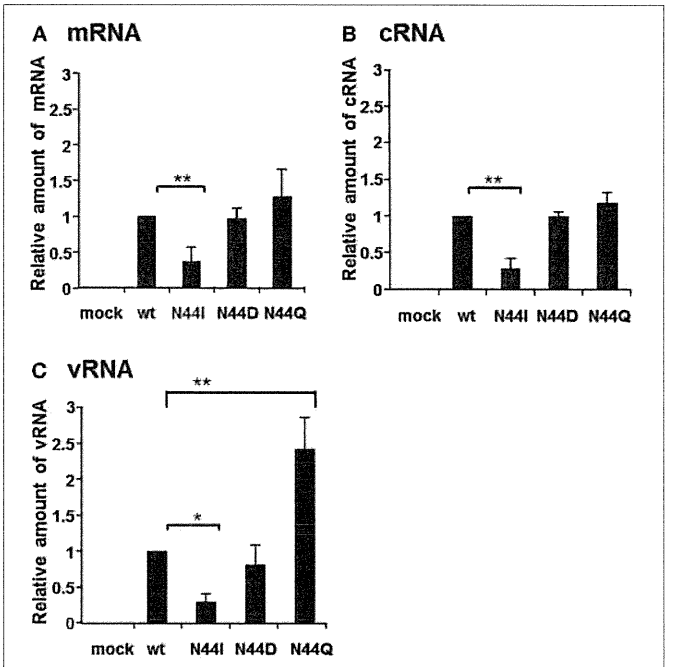

FIGURE 5 | RNA synthesis of viruses containing mutations at the amino acid position 44. Wild-type virus and mutant viruses containing amino acids N and I, D, and Q, respectively, at the a.a. position 44 were infected into MDCK cells at MOI of 2.5. At 9 hpi, the accumulation levels of viral mRNA **(A)**, cRNA **(B)**, and vRNA **(C)** were measured by qRT-PCR, and the amounts of these RNAs were normalized by that of cellular actin mRNA. These results are averages from three independent experiments with standard deviations. $^{*}p < 0.05$; $^{**}p < 0.01$.

Thus, it is expected that the a.a. position 44 might be a water-soluble characteristic, and especially glutamine at this position stimulates the vRNA synthesis.

DISCUSSION

In this report, we have studied on three a.a. positions, i. e., 16, 27, and 44, which are not conserved between influenza A and B viruses. The RNA synthesis activity of D27V was enhanced, while that of N44I was decreased (**Figure 2**). Based on these, we carried out further mutational analyses. The N44I showed the decreased level of RNA synthesis in three types of viral RNAs, while N44D did not affect the RNA synthesis (**Figure 5**). Interestingly, N44Q increased vRNA synthesis with little effect on viral mRNA and cRNA synthesis. It is possible that side chain group of Q may stimulate the cRNA promoter binding and increase the vRNA synthesis activity.

D27V and D27N increased the RNA synthesis, while D27E mutation gave no effects (**Figure 4**). Furthermore, when the amounts of RNAs of D27V were analyzed at various MOI, those of D27V were increased (Figure S3). Although uncharged amino acid at this position enhances the RNA synthesis, molecular evolution has selected negatively charged amino acids. Therefore, it is assumed that charged amino acids at this position, even with low efficiency for the replication, are needed for PB1. Recently, mutational analyses showed that the sequences surrounding the PB1 AUG codon are multifunctional, and contain overlapping signals for translation initiation and for segment specific packaging (Wise et al., 2011). We may consider a possibility that there is some regulatory coupling between replication and packaging and the a.a. position 27 has a role in this hypothetical mechanism.

These a.a. positions are close to the PA binding site, and the PB1-RNA interaction could be affected by the presence of PA. We examined whether these mutations affect the assembly of

RdRp (Figure S1). The assembly of PB1 with PA and PB2 was not affected by these mutations. Moreover, these mutations did not affect the transcription activity, mRNA synthesis from vRNA (**Figure 3** and Figure S2). Taken altogether, it is quite likely that amino acids at the positions 27 and 44 are involved in the replication activity, possibly in cRNA promoter recognition with little effects on the transcription activity and the assembly of the RdRp complex.

Recognition of the vRNA promoter depends on the 5′-arm of the promoter and this binding improves the weak binding of RdRp to the 3′-arm of the vRNA promoter (Tiley et al., 1994; Gonzalez and Ortin, 1999a; Jung and Brownlee, 2006). Recognition of the cRNA promoter by RdRp has been shown by the *in vitro* binding of the PB1 subunit with the 5′- and 3′-arms of the cRNA promoter (Gonzalez and Ortin, 1999b). Flexibility within the two uridines of the internal loop of the cRNA promoter required for protein binding in the cRNP complex (Park et al., 2003). Biochemical studies have shown that conformational changes in PB1 of the influenza A virus RdRp lead to the interaction with either vRNA or cRNA (Gonzalez and Ortin, 1999b). Based on previous reports and our findings, the positions 27 and 44 may affect the PB1 structure, resulting in affecting PB1 binding activity to the 3′-arm of the cRNA promoter. Thus, we would propose that these positions in PB1 are important for the replication activity by recognizing the cRNA promoter.

ACKNOWLEDGMENTS

This research was supported in part by a grant-in-aid from the Ministry of Education, Culture, Sports, Science, and Technology of Japan (to Kyosuke Nagata).

SUPPLEMENTARY MATERIAL

The Supplementary Material for this article can be found online at: http://www.frontiersin.org/journal/10.3389/fmicb.2013.00398/abstract

REFERENCES

Asano, Y., and Ishihama, A. (1997). Identification of two nucleotide-binding domains on the PB1 subunit of influenza virus RNA polymerase. *J. Biochem.* 122, 627–634. doi: 10.1093/oxfordjournals.jbchem.a021799

Biswas, S. K., and Nayak, D. P. (1996). Influenza virus polymerase basic protein 1 interacts with influenza virus polymerase basic protein 2 at multiple sites. *J. Virol.* 70, 6716–6722.

Gonzalez, S., and Ortin, J. (1999a). Characterization of influenza virus PB1 protein binding to viral RNA: two separate regions of the protein contribute to the interaction domain. *J. Virol.* 73, 631–637.

Gonzalez, S., and Ortin, J. (1999b). Distinct regions of influenza virus PB1 polymerase subunit recognize vRNA and cRNA templates. *EMBO J.* 18, 3767–3775. doi: 10.1093/emboj/18.13.3767

Gonzalez, S., Zurcher, T., and Ortin, J. (1996). Identification of two separate domains in the influenza virus PB1 protein involved in the interaction with the PB2 and PA subunits: a model for the viral RNA polymerase structure. *Nucleic Acids Res.* 24, 4456–4463. doi: 10.1093/nar/24.22.4456

He, X., Zhou, J., Bartlam, M., Zhang, R., Ma, J., Lou, Z., et al. (2008). Crystal structure of the polymerase PA(C)-PB1(N) complex from an avian influenza H5N1 virus. *Nature* 454, 1123–1126. doi: 10.1038/nature07120

Jung, T. E., and Brownlee, G. G. (2006). A new promoter-binding site in the PB1 subunit of the influenza A virus polymerase. *J. Gen. Virol.* 87, 679–688. doi: 10.1099/vir.0.81453-0

Kawaguchi, A., and Nagata, K. (2007). De novo replication of the influenza virus RNA genome is regulated by DNA replicative helicase, MCM. *EMBO J.* 26, 4566–4575. doi: 10.1038/sj.emboj.7601881

Kawaguchi, A., Naito, T., and Nagata, K. (2005). Involvement of influenza virus PA subunit in assembly of functional RNA polymerase complexes. *J. Virol.* 79, 732–744. doi: 10.1128/JVI.79.2.732-744.2005

Kolpashchikov, D. M., Honda, A., and Ishihama, A. (2004). Structure-function relationship of the influenza virus RNA polymerase: primer-binding site on the PB1 subunit. *Biochemistry* 43, 5882–5887. doi: 10.1021/bi036139e

Li, M. L., Ramirez, B. C., and Krug, R. M. (1998). RNA-dependent activation of primer RNA production by influenza virus polymerase: different regions of the same protein subunit constitute the two required RNA-binding sites. *EMBO J.* 17, 5844–5852. doi: 10.1093/emboj/17.19.5844

Nagata, K., Kawaguchi, A., and Naito, T. (2008). Host factors for replication and transcription of the influenza virus genome. *Rev. Med. Virol.* 18, 247–260. doi: 10.1002/rmv.575

Neumann, G., Watanabe, T., Ito, H., Watanabe, S., Goto, H., Gao, P., et al. (1999). Generation of influenza A viruses entirely from cloned cDNAs. *Proc. Natl. Acad. Sci. U.S.A.* 96, 9345–9350. doi: 10.1073/pnas.96.16.9345

Obayashi, E., Yoshida, H., Kawai, F., Shibayama, N., Kawaguchi, A., Nagata, K., et al. (2008). The structural basis for an essential subunit interaction in influenza virus RNA polymerase. *Nature* 454, 1127–1131. doi: 10.1038/nature07225

Ohtsu, Y., Honda, Y., Sakata, Y., Kato, H., and Toyoda, T. (2002). Fine mapping of the subunit binding sites of influenza virus RNA polymerase. *Microbiol. Immunol.* 46, 167–175. doi: 10.1111/j.1348-0421.2002.tb02682.x

Park, C. J., Bae, S. H., Lee, M. K., Varani, G., and Choi, B. S. (2003). Solution structure of the influenza A virus cRNA promoter: implications for differential recognition of viral promoter structures by RNA-dependent RNA polymerase. *Nucleic Acids Res.* 31, 2824–2832. doi: 10.1093/nar/gkg387

Sugiyama, K., Obayashi, E., Kawaguchi, A., Suzuki, Y., Tame, J. R., Nagata, K., et al. (2009). Structural insight into the essential PB1-PB2 subunit contact of the influenza virus RNA polymerase. *EMBO J.* 28, 1803–1811. doi: 10.1038/emboj.2009.138

Taubenberger, J. K., Reid, A. H., Lourens, R. M., Wang, R., Jin, G., and Fanning, T. G. (2005). Characterization of the 1918 influenza virus polymerase genes. *Nature* 437, 889–893. doi: 10.1038/nature04230

Tiley, L. S., Hagen, M., Matthews, J. T., and Krystal, M. (1994). Sequence-specific binding of the influenza virus RNA polymerase to sequences located at the 5′ ends of the viral RNAs. *J. Virol.* 68, 5108–5116.

Toyoda, T., Adyshev, D. M., Kobayashi, M., Iwata, A., and Ishihama, A. (1996). Molecular assembly of the influenza virus RNA polymerase: determination of the subunit-subunit contact sites. *J. Gen. Virol.* 77 (pt 9), 2149–2157. doi: 10.1099/0022-1317-77-9-2149

Vreede, F. T., Jung, T. E., and Brownlee, G. G. (2004). Model suggesting that replication of influenza virus is regulated by stabilization of replicative intermediates. *J. Virol.* 78, 9568–9572. doi: 10.1128/JVI.78.17.9568-9572.2004

Wise, H. M., Barbezange, C., Jagger, B. W., Dalton, R. M., Gog, J. R., Curran, M. D., et al. (2011). Overlapping signals for translational regulation and packaging of influenza A virus segment 2. *Nucleic Acids Res.* 39, 7775–7790. doi: 10.1093/nar/gkr487

Zurcher, T., de La Luna, S., Sanz-Ezquerro, J. J., Nieto, A., and Ortin, J. (1996). Mutational analysis of the influenza virus A/Victoria/3/75 PA protein: studies of interaction with PB1 protein and identification of a dominant negative mutant. *J. Gen. Virol.* 77 (pt 8), 1745–1749. doi: 10.1099/0022-1317-77-8-1745

Conflict of Interest Statement: The authors declare that the research was conducted in the absence of any commercial or financial relationships that could be construed as a potential conflict of interest.

Received: 17 October 2013; accepted: 04 December 2013; published online: 18 December 2013.

Citation: Binh NT, Wakai C, Kawaguchi A and Nagata K (2013) The N-terminal region of influenza virus polymerase PB1 adjacent to the PA binding site is involved in replication but not transcription of the viral genome. Front. Microbiol. 4:398. doi: 10.3389/fmicb.2013.00398

This article was submitted to Virology, a section of the journal Frontiers in Microbiology.

SCIENTIFIC REPORTS

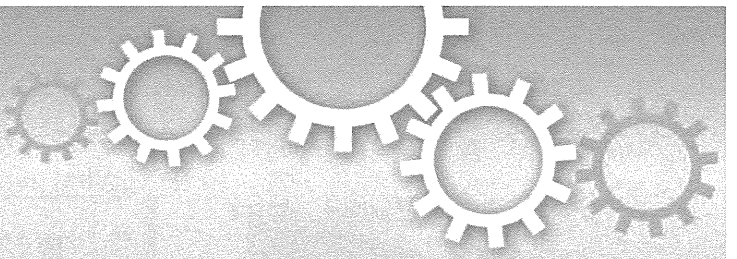

OPEN

SUBJECT AREAS:
VIRAL PROTEINS
CHROMOSOMES
ADENOVIRUS
CHROMATIN STRUCTURE

Received
13 May 2013

Accepted
25 June 2013

Published
15 July 2013

Correspondence and requests for materials should be addressed to K.N. (knagata@md.tsukuba.ac.jp)

DNA replication-dependent binding of CTCF plays a critical role in adenovirus genome functions

Tetsuro Komatsu[1,2], Takeshi Sekiya[1] & Kyosuke Nagata[1]

[1]Department of Infection Biology, Faculty of Medicine and Graduate School of Comprehensive Human Sciences, University of Tsukuba, Tsukuba 305-8575, Japan, [2]Microbiologie Fondamentale et Pathogénicité, MFP CNRS UMR 5234, Université Bordeaux SEGALEN, Bordeaux 33076, France.

The expression of adenovirus late genes is shown to require viral DNA replication, but its mechanism remains elusive. Here we found that knockdown of CTCF suppresses viral DNA replication as well as late, but not early, gene expression. Chromatin immunoprecipitation assays indicated that CTCF binds to viral chromatin depending on viral DNA replication. These findings depict CTCF as a critical regulator for adenovirus genome functions in late phases of infection.

In the cell nucleus, the genomic DNA forms chromatin structure. It is being clarified that the higher-order chromatin structure, such as the DNA looping, plays an important role in a dynamic property of the chromatin[1]. One of the chromatin organizing proteins, CTCF (CCCTC-binding factor), is a well-characterized chromatin-binding factor involved in the formation of the long-range interactions of chromatin[2]. CTCF has eleven zinc fingers and therefore binds to divergent DNA sequences, as indicated by chromatin immunoprecipitation (ChIP) in combination with tiling arrays (ChIP-on-chip)[3] or high-throughput sequencing analyses (ChIP-seq)[4]. A variety of chromatin-related proteins are reported as binding partners of CTCF, including cohesin complexes[5,6], a nucleolar protein B23/nucleophosmin, and CTCF itself[7]. These interactions are thought to enable CTCF binding sites to contact each other and/or be tethered to the subnuclear domains, resulting in the formation of intra- and interchromatin interaction[2]. In addition to the role on the cellular chromatin, recent reports have revealed the involvement of CTCF on viral proliferation, as Lieberman and co-workers recently demonstrated the CTCF-mediated formation of chromatin loops on Kaposi's sarcoma-associated Herpesvirus (KSHV) and Epstein-Barr virus (EBV) genomes[8,9]. It is shown that CTCF regulates the latency-specific chromatin conformation of KSHV and EBV genomes, and siRNA-mediated depletion of CTCF or mutations in the CTCF binding sites disrupt the chromatin architecture and de-regulate latent gene expression[8,9]. Thus, CTCF could impact on the regulation of not only cellular but also viral chromatin.

The adenovirus (Ad) has a linear double-stranded DNA genome that forms chromatin-like structure in the virion[10]. Previously, we have reported that viral chromatin structure regulates the expression of viral early genes (e.g. E1A, E4 genes) in early phases of infection[11,12]. The expression of the late genes (e.g. major late genes) are hardly observed during early phases of infection, while concomitantly with the onset of viral DNA replication, those genes are fully activated. Thomas and Mathews demonstrated that the expression of the late genes requires viral DNA replication in *cis*[13]. In addition, we have shown the regulatory mechanism of the viral chromatin structure during DNA replication and proposed a possible role of viral DNA replication in the activation of late genes[14]. Thus, it is suggested that the regulation of viral chromatin structure has a significant role in the DNA replication-dependent activation of viral genes. In spite of these evidences, however, the functional relationship between viral gene expression and DNA replication in infected cells remains largely unclear. In this study we sought to further clarify the role of chromatin structure and/or chromatin-related factors on the Ad genome DNA. As described above, it is shown that CTCF plays a role on the chromatin of some DNA viruses[8,9]. These lead us to hypothesize that CTCF could function also on Ad chromatin.

Results

CTCF is required for viral DNA replication and late gene expression. To study a role of CTCF, we carried out knock down (KD) of the expression of CTCF by siRNA treatment (Fig. 1A). Either control siRNA (siCont) or

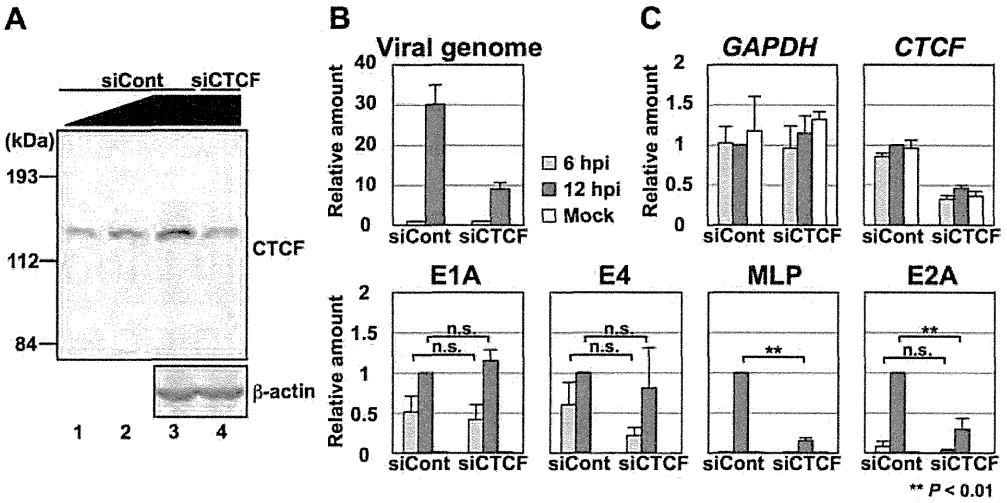

Figure 1 | Effects of CTCF KD on viral DNA replication and gene expression. (A) Western blotting and knockdown of CTCF. Cell lysates were prepared from HeLa cells treated with siCont (lanes 3) or siCTCF (lane 4) and subjected to western blot analyses using anti-CTCF (top panel) and anti-β-actin antibodies (bottom panel). For siCont-treated cells, 25% (lane 1) and 50% (lane 2) volume of lysates were also loaded. Full-size images are shown in Supplementary figure 1. (B) Amounts of viral DNA. HeLa cells treated with siCont or siCTCF were infected with HAdV5 at an MOI of 100, and total DNAs were purified at 6 and 12 hpi. The amount of viral DNA was measured by qPCR using primers for the E1A promoter. The amount at 12 hpi relative to that at 6 hpi was graphed. Mean values with s.d. were obtained from three independent experiments. (C) RT-qPCR assays. Total RNAs were purified at 6 and 12 hpi, and subjected to RT-qPCR using indicated primer sets. The mRNA levels relative to those of control cells at 12 hpi were graphed. Mean values with s.d. were obtained from three independent experiments. *P*-values are calculated using Student's *t*-test. "n.s." indicates "not statistically significant".

siRNA targeted for CTCF (siCTCF) was introduced into HeLa cells, and then cell lysates were prepared and subjected to western blot analyses using anti-CTCF antibody. Only a single band corresponding to CTCF was detected, demonstrating the specificity of the antibody. Under our experimental condition, the expression level of CTCF in siCTCF-treated cells was decreased to approximately 25% of that in control cells (Fig. 1A, compare lane 4 with lanes 1–3).

To test whether CTCF plays a role in Ad DNA replication and gene expression, we carried out CTCF KD followed by quantitative PCR (qPCR) of viral DNA and RT-qPCR (Fig. 1B and C). Under our experimental condition, the onset of viral DNA replication can be observed around 8 hpi (hours post infection)[12,14]. siCont- or siCTCF-treated cells were mock-infected or infected with human adenovirus type 5 (HAdV5) at an MOI (multiplicity of infection) of 100, and at 6 (for early phases) and 12 hpi (for late phases of infection) total DNAs and RNAs were purified. We first measured viral DNA amounts by qPCR using a primer set targeted for the E1A promoter region (E1A pro, see Table 2) to evaluate the efficiency of viral DNA replication (Fig. 1B). In siCont-treated cells, the amount of viral DNA was increased by ~30 fold through viral DNA replication. In contrast, siCTCF-treated cells allowed only ~9 fold amplification of viral DNA.

Next, we performed RT-qPCR assays using several primer sets for cellular and viral genes (Fig. 1C). Under the condition employed here, the mRNA level of *GAPDH* was unaffected by Ad infection and siRNA treatment, and that of *CTCF* was specifically decreased by siCTCF treatment (Fig. 1C, *GAPDH* and *CTCF*). The mRNA levels of viral early genes were not significantly affected by CTCF KD (Fig. 1C, E1A and E4), suggesting that CTCF is not involved in viral early gene expression. In contrast, the level of mRNA transcribed from the major late promoter (MLP) was drastically decreased by siCTCF treatment (Fig. 1C, MLP). Similarly, the mRNA level of E2A was reduced by CTCF KD, particularly at 12 hpi (Fig. 1C, E2A). It is noted that E2 gene transcription is regulated by early and late promoters and transcription from the E2 late promoter depends on viral DNA replication[15] (Unpublished data). Therefore, it is reasonable to assume that CTCF KD could predominantly affect the transcription from the E2 late promoter, although in this study we did not discriminate E2A mRNAs transcribed from two promoters. Collectively, these results suggest that CTCF is critical for viral DNA replication as well as late, but not early, gene expression.

CTCF binds to viral chromatin in a DNA replication-dependent manner. To examine whether CTCF functions directly on viral chromatin, ChIP assays were performed using anti-CTCF antibody (Fig. 2). Since the effect of CTCF KD was observed in late phases of infection (Fig. 1), first we studied using infected cells at 12 hpi for ChIP assays (Fig. 2A). We used a variety of primer sets for the Ad genome to test the genome-wide binding of CTCF (see Fig. 2B). We found that CTCF is recruited into several regions of the virus genome, including the MLP region and the ORF regions of the viral structural protein (Hexon) and the E4 ORF3 gene (E4 orf). In addition, a weak binding of CTCF at the E1A pro region was observed. Next, we focused on three CTCF binding sites, the E1A pro, MLP, and Hexon regions, and performed ChIP assays using cells cultured in the absence or presence of hydroxyurea (HU), a DNA replication inhibitor, to examine whether the CTCF binding observed here is DNA replication-dependent (Fig. 2C). The recruitment of CTCF into those regions was observed only at 12 hpi, and this was inhibited by the addition of HU, indicating that CTCF is recruited onto viral chromatin in a DNA replication-dependent manner.

Discussion

The results obtained in this study indicate that CTCF binds to Ad chromatin depending on its DNA replication and plays a pivotal role in late phases of infection. Our KD experiments clearly reveal that CTCF is required for viral DNA replication and late gene expression (Fig. 1B and C). It is demonstrated that viral late genes are activated depending on its DNA replication[13]. Thus, the mRNA levels of late genes also should be affected when only DNA replication would be directly repressed by CTCF KD. Conversely, viral factors involved in

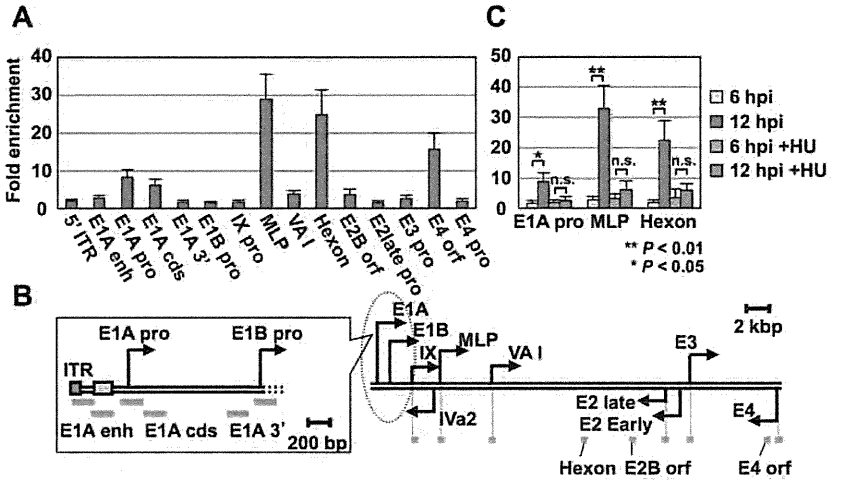

Figure 2 | CTCF binding on viral chromatin. (A) ChIP assays with anti-CTCF antibody. HeLa cells were infected with HAdV5 at an MOI of 100, and at 12 hpi subjected to ChIP assays using anti-CTCF and anti-FLAG antibodies. The binding levels were calculated as fold enrichment against that obtained in a negative control (anti-FLAG antibody). Mean values with s.d. were obtained from three independent experiments. (B) Structure of the Ad genome. Arrows represent promoters of viral genes. Target regions for ChIP assays are indicated by gray bars. (C) Effect of viral DNA replication on CTCF binding. HeLa cells were infected with HAdV5 and cultured in the absence or presence of 2 mM HU. At 6 and 12 hpi, ChIP assays were carried out as described above. *P*-values are calculated using Student's *t*-test.

its DNA replication are encoded by the E2 gene, and its expression was suppressed by CTCF KD (Fig. 1C). Therefore, the inhibition of viral late gene expression also could be the cause for less efficient viral DNA replication. Because of this interdependency, we could not precisely discriminate whether CTCF KD primarily affects viral DNA replication or late gene expression (or both). In addition, we could not exclude the possibility that the lower level of the MLP mRNA in siCTCF-treated cells results from less amount of viral DNA templates due to the defect in viral DNA replication. Nonetheless, we speculate that CTCF may be involved in the regulation of late gene expression: First, the binding of CTCF is dependent on viral DNA replication (Fig. 2C), suggesting that this protein possibly functions in the step(s) later than viral DNA replication; second, when the level of the MLP mRNA at 12 hpi was normalized by the amounts of the virus genome, the level of the MLP mRNA per one viral DNA in CTCF KD cells was still lower than that in control cells (Fig. 1, MLP mRNA level: ~15%/virus genome: ~30% = MLP mRNA per one viral DNA: ~50%).

It is an important question how CTCF regulates the function of the virus genome/chromatin. Although in this study we found several CTCF binding sites (Fig. 2A), there could be additional regions for CTCF on the virus genome. Thus, at the moment, it is difficult to dissect a role of each CTCF binding site and the cooperative function among those regions. It is suggested that the E1B, IX, and E2 late genes/promoters are also activated depending on viral DNA replication[15–17] as is the MLP. However, we could not observe the CTCF binding on those regions (Fig. 2A), suggesting that the recruitment of CTCF onto each late promoter seems not to be required for the genome-wide coordination between viral DNA replication and the expression of late genes. Further studies are needed to address these points. As described above, it is shown that Ad DNA replication is required for the activation of viral late genes[13]. Similarly it is reported that DNA replication is essential for the expression of certain cellular genes such as the *HoxB* gene[18], although the molecular details remain to be determined. To our knowledge, this is the first report indicating the possible involvement of CTCF in the DNA replication-dependent activation of the genes. Thus, our findings may provide insight into an uncharacterized mechanism of gene regulation that involves DNA replication.

Methods

Cells and viruses. Maintenance of HeLa cells, and purification and infection of human adenovirus type 5 (HAdV5) were carried out essentially as described previously[12,14]. Hydroxyurea (HU) was added at the final concentration of 2 mM right after infection to block DNA replication.

Antibodies. To obtain recombinant CTCF N-terminal region (amino acids (aa) 1–267) as an antigen, the expression vector for His-tagged CTCF(1–267) was constructed. cDNA fragment of full-length CTCF was amplified by PCR with a primer set, 5′-AGGGCATATGGAAGGTGATGCAGTCGAAGCCATTGTGG-3′ and 5′-AGCCTCGAGAAGTCCTGGCGACGCACAAGGCTCCGCC-3′, and cloned into the pBluescript-FLAG vector (pBS-FLAG-CTCF). Using pBS-FLAG-CTCF as a template, cDNA fragment corresponding to aa 1-267 was amplified by PCR with a primer set, 5′-AGGGCATATGGAAGGTGATGCAGTCGAAG-CCATTGTGG-3′ and 5′-GTTGAATTCACTGGAATGTCTTCTTTACAC-3′, and cloned into the pET-14b vector. *E. coli* was transformed with the resultant vector, pET-14b-CTCF(1-267), and His-CTCF(1–267) was expressed and purified using the Ni-NTA resin (Novagen) according to the manufacturer's protocol.

Rabbit anti-CTCF antibody was raised against His-CTCF(1–267) according to standard protocols. Mouse anti-FLAG M2 and mouse anti-β-actin antibodies were described elsewhere[12,14].

RT-qPCR assays. RT-PCR and quantitative PCR (qPCR) were performed essentially as described previously[12,14]. Total RNAs were purified by phenol extraction followed by DNase I treatment. cDNA was synthesized from total RNA (1 μg) using ReverTraAce (Toyobo) and oligo-dT primer according to the manufacturer's protocol. qPCR was carried out using FastStart SYBR Green Master (Roche) and

Table 1 | Primers used for RT-qPCR

Primer	Sequence (5′-3′)
GAPDH forward	AGCCAAAAGGGTCATCATCTC
GAPDH reverse	GGACTGTGGTCATGAGTCCTTC
CTCF forward	TGACACAGTCATAGCCCGAAAA
CTCF reverse	TGCCTTGCTCAATATAGGAATGC
E1A forward	GAGACATATTATCTGCCACGGAG
E1A reverse	AGTGAGTAAGTCAATCCCTTCCTG
E4 forward	ACAGAACCCTAGTATTCAACCTGC
E4 reverse	GACAGCGACATGAACTTAAGTGAG
MLP forward	ACTCTCTTCCGCATCGCTGT
MLP reverse	GTGACTGGTTAGACGCCTTTCT
E2A forward	GTGTAGACACTTAAGCTCGCCTT
E2A reverse	CTTCAAACTACTGCCTGACCAAGT

Table 2 | Primers used for ChIP

Primer	Sequence (5′-3′)
5′ inverted terminal region forward	CAATATGATAATGAGGGGGTGG
5′ inverted terminal region reverse	ACTACAACATCCGCCTAAAACC
E1A enhancer region forward	CGGTGTACACAGGAAGTGACAAT
E1A enhancer region reverse	AGTCTCCACGTAAACGGTCAAAGT
E1A promoter region forward	GGGTCAAAGTTGGCGTTTTA
E1A promoter region reverse	CAAAATGGCTAGGAGGTGGA
E1A coding region forward	GAGACATATTATCTGCCACGGAG
E1A coding region reverse	AGTGAGTAAGTCAATCCCTTCCTG
E1A 3′ region forward	CCTTCTAACACACCTCCTGAGATAC
E1A 3′ region reverse	ACACACGCAATCACAGGTTTAC
E1B promoter region forward	GTGTGTGGTTAACGCCTTTGT
E1B promoter region reverse	GAGGTACTGTTAGAGCTCTGTTCCA
IX promoter region forward	GGCTCTAGCGATGAAGATACAGAT
IX promoter region reverse	CATCACATTCTGACGCACCC
ML promoter region forward	AGGTGATTGGTTTGTAGGTGTAGG
ML promoter region reverse	CTCCTCGTTTTTGGAAACTGAC
VA I gene region forward	GTGCAAAAGGAGAGCCTGTAAG
VA I gene region reverse	AGGAAGCCAAAAGGAGCACT
Hexon ORF region forward	CGCAGTGGTCTTACATGCAC
Hexon ORF region reverse	CACACGGTTATCACCCACAG
E2B ORF region forward	AGAAGAACATGCCGCAAGAC
E2B ORF region reverse	TCGAAGGCGAGCTTAAGTGT
E2 late promoter region forward	ATTATCGGTACCTTTGAGCTGC
E2 late promoter region reverse	AGAATGTGGCCCTGGGTAAT
E3 promoter region forward	AAGTTCAGATGACTAACTCAGGGG
E3 promoter region reverse	AGAGTTAGGATTGCCTGACGAG
E4 ORF3 region forward	TGGCGTGGTCAAACTCTACA
E4 ORF3 region reverse	GATTTTTACAATGGCCGGACT
E4 promoter region forward	CCATAACAGTCAGCCTTACCAGT
E4 promoter region reverse	GTGACGATTTGAGGAAGTTGTG

Thermal Cycler Dice Real Time System (Takara) according to the manufacturers' protocol.

Table 1 indicates primer sequences for *GAPDH*, *CTCF*, E1A, E4, MLP, and E2A genes.

ChIP assays. ChIP assays were carried out according to the protocol from Chromatin Immunoprecipitation Assay Kit (Millipore) with minor modification, essentially as described previously[12,14]. Briefly, cells were fixed with 1% formaldehyde, followed by the addition of glycine at the final concentration of 125 mM for quenching. After centrifugation, cell pellets were lysed with SDS lysis buffer (50 mM Tris-HCl [pH 7.9], 10 mM EDTA, and 1% SDS), and lysates were subjected to sonication to shear the chromatin DNA to ~1 kbp in size. Sonicated samples were diluted 10 fold with ChIP dilution buffer (16.7 mM Tris-HCl [pH 7.9], 1.2 mM EDTA, 167 mM NaCl, 1.1% Triton X-100, and 0.01% SDS) and then pre-cleared with Protein A Sepharose 4 Fast Flow (GE Healthcare). An antibody was added to the pre-cleared sample solution and incubated overnight at 4°C. Antibody-protein-DNA complexes were incubated with Protein A Sepharose at 4°C for 1 hr, and then the beads were washed with Low Salt Wash Buffer (20 mM Tris-HCl [pH 7.9], 2 mM EDTA, 150 mM NaCl, 1% Triton X-100, and 0.1% SDS), High Salt Wash Buffer (20 mM Tris-HCl [pH 7.9], 2 mM EDTA, 500 mM NaCl, 1% Triton X-100, and 0.1% SDS), LiCl Wash Buffer (10 mM Tris-HCl [pH 7.9], 1 mM EDTA, 0.25 M LiCl, 1% NP-40, and 1% deoxycholic acid), and TE (10 mM Tris-HCl [pH 7.9] and 1 mM EDTA) successively. Protein-DNA complexes were eluted from the beads with elution buffer (1% SDS, 100 mM $NaHCO_3$, and 10 mM DTT), and crosslinking was reversed by incubation at 65°C for 4 hr. After treatment with Proteinase K, DNAs were recovered by phenol/chloroform extraction and ethanol precipitation. Obtained DNA samples were subjected to qPCR as described above.

Table 2 shows primer sequences for 5′ inverted terminal region (5′ ITR), the E1A enhancer (E1A enh), the E1A promoter (E1A pro), the E1A coding region (E1A cds), the E1A 3′ region (E1A 3′), the E1B promoter (E1B pro), the IX promoter (IX pro), the ML promoter (MLP), the VA I gene (VA I), the Hexon ORF (Hexon), the E2B ORF (E2B orf), the E2 late promoter (E2late pro), the E3 promoter (E3 pro), the E4 ORF3 (E4 orf), and the E4 promoter regions (E4 pro).

siRNA-mediated knockdown, quantification of viral DNA, and western blot assays. These experiments were carried out essentially as described previously[12,14,19]. siRNA targeted for CTCF was commercially purchased (Stealth siRNA; Invitrogen). siRNAs were introduced into cells with Lipofectamine 2000 (Invitrogen) according to the manufacturer's protocol. Total DNAs were purified by treatment with Proteinase K, followed by phenol/chloroform extraction and ethanol precipitation, as described previously[19]. Quantitative determination of viral DNA was carried out by qPCR as described above. For western blot analyses, cell lysates were subjected to SDS-PAGE, and proteins were transferred to a PVDF membrane (Millipore). The membrane was incubated with primary antibodies, followed by incubation with secondary antibodies conjugated with horseradish peroxidase (GE Healthcare). The blot was developed using Chemi-Lumi One (Nacalai tesque).

1. Raab, J. R. & Kamakaka, R. T. Insulators and promoters: closer than we think. *Nat Rev Genet* **11**, 439–46 (2010).
2. Phillips, J. E. & Corces, V. G. CTCF: master weaver of the genome. *Cell* **137**, 1194–211 (2009).
3. Kim, T. H. *et al.* Analysis of the vertebrate insulator protein CTCF-binding sites in the human genome. *Cell* **128**, 1231–45 (2007).
4. Barski, A. *et al.* High-resolution profiling of histone methylations in the human genome. *Cell* **129**, 823–37 (2007).
5. Stedman, W. *et al.* Cohesins localize with CTCF at the KSHV latency control region and at cellular c-myc and H19/Igf2 insulators. *EMBO J* **27**, 654–66 (2008).
6. Wendt, K. S. *et al.* Cohesin mediates transcriptional insulation by CCCTC-binding factor. *Nature* **451**, 796–801 (2008).
7. Yusufzai, T. M., Tagami, H., Nakatani, Y. & Felsenfeld, G. CTCF tethers an insulator to subnuclear sites, suggesting shared insulator mechanisms across species. *Mol Cell* **13**, 291–8 (2004).
8. Kang, H., Wiedmer, A., Yuan, Y., Robertson, E. & Lieberman, P. M. Coordination of KSHV latent and lytic gene control by CTCF-cohesin mediated chromosome conformation. *PLoS Pathog* **7**, e1002140 (2011).
9. Tempera, I., Klichinsky, M. & Lieberman, P. M. EBV latency types adopt alternative chromatin conformations. *PLoS Pathog* **7**, e1002180 (2011).
10. Giberson, A. N., Davidson, A. R. & Parks, R. J. Chromatin structure of adenovirus DNA throughout infection. *Nucleic Acids Res* **40**, 2369–76 (2012).
11. Haruki, H., Okuwaki, M., Miyagishi, M., Taira, K. & Nagata, K. Involvement of template-activating factor I/SET in transcription of adenovirus early genes as a positive-acting factor. *J Virol* **80**, 794–801 (2006).
12. Komatsu, T., Haruki, H. & Nagata, K. Cellular and viral chromatin proteins are positive factors in the regulation of adenovirus gene expression. *Nucleic Acids Res* **39**, 889–901 (2011).
13. Thomas, G. P. & Mathews, M. B. DNA replication and the early to late transition in adenovirus infection. *Cell* **22**, 523–33 (1980).
14. Komatsu, T. & Nagata, K. Replication-uncoupled histone deposition during adenovirus DNA replication. *J Virol* **86**, 6701–11 (2012).
15. Swaminathan, S. & Thimmapaya, B. Regulation of adenovirus E2 transcription unit. *Curr Top Microbiol Immunol* **199**, 177–94 (1995).
16. Matsui, T., Murayama, M. & Mita, T. Adenovirus 2 peptide IX gene is expressed only on replicated DNA molecules. *Mol Cell Biol* **6**, 4149–54 (1986).

17. Maxfield, L. F. & Spector, D. J. Readthrough activation of early adenovirus E1b gene transcription. *J Virol* **71**, 8321–9 (1997).
18. Fisher, D. & Méchali, M. Vertebrate HoxB gene expression requires DNA replication. *EMBO J* **22**, 3737–48 (2003).
19. Samad, M. A., Komatsu, T., Okuwaki, M. & Nagata, K. B23/nucleophosmin is involved in regulation of adenovirus chromatin structure at late infection stages, but not in virus replication and transcription. *J Gen Virol* **93**, 1328–38 (2012).

Acknowledgments

This work was supported in part by grants-in-aid for scientific research from the Ministry of Education, Culture, Sports, Science, and Technology of Japan (to K.N.).

Author contributions

T.K. and K.N. designed the study; T.K. and T.S. performed the experiments; T.K. and K.N. prepared the manuscript; All authors reviewed the manuscript.

Additional information

Supplementary information accompanies this paper at http://www.nature.com/scientificreports

Competing financial interests: The authors declare no competing financial interests.

How to cite this article: Komatsu, T., Sekiya, T. & Nagata, K. DNA replication-dependent binding of CTCF plays a critical role in adenovirus genome functions. *Sci. Rep.* **3**, 2187; DOI:10.1038/srep02187 (2013).

J Nat Med
DOI 10.1007/s11418-012-0725-0

ORIGINAL PAPER

Anti-influenza virus activity of *Ginkgo biloba* leaf extracts

Takahiro Haruyama · Kyosuke Nagata

Received: 27 July 2012 / Accepted: 9 November 2012

Abstract We examined the influence of *Ginkgo biloba* leaf extract (EGb) on the infectivity of influenza viruses in Madin–Darby canine kidney (MDCK) cells. Plaque assays demonstrated that multiplication of influenza viruses after adsorption to host cells was not affected in the agarose overlay containing EGb. However, when the viruses were treated with EGb before exposure to cells, their infectivity was markedly reduced. In contrast, the inhibitory effect was not observed when MDCK cells were treated with EGb before infection with influenza viruses. Hemagglutination inhibition assays revealed that EGb interferes with the interaction between influenza viruses and erythrocytes. The inhibitory effect of EGb was observed against influenza A (H1N1 and H3N2) and influenza B viruses. These results suggest that EGb contains an anti-influenza virus substance(s) that directly affects influenza virus particles and disrupts the function of hemagglutinin in adsorption to host cells. In addition to the finding of the anti-influenza virus activity of EGb, our results demonstrated interesting and important insights into the screening system for anti-influenza virus activity. In general, the plaque assay using drug-containing agarose overlays is one of the most reliable methods for detection of antiviral activity. However, our results showed that EGb had no effects either on the number of plaques or on their sizes in the plaque assay. These findings suggest the existence of inhibitory activities against the influenza virus that were overlooked in past studies.

Keywords Antiviral effect · *Ginkgo biloba* leaf extract · Hemagglutination · Influenza virus

T. Haruyama · K. Nagata (✉)
Department of Infection Biology, Faculty of Medicine and Graduate School of Comprehensive Human Sciences, University of Tsukuba, 1-1-1 Tennodai, Tsukuba 305-8575, Japan
e-mail: knagata@md.tsukuba.ac.jp

Present Address:
T. Haruyama
Research Center, AVSS Corporation, 1-22 Wakaba-machi, Nagasaki 852-8137, Japan

Introduction

Influenza viruses, members of the *Orthomyxoviridae* family, cause epidemics in the human population every year despite the availability of effective vaccines. In a severe pandemic year, millions of people die from the infection. Influenza viruses are classified on the basis of the antigenic properties of two surface glycoproteins: hemagglutinin (HA) and neuraminidase (NA). Sixteen HA subtypes (H1–H16) and nine NA subtypes (N1–N9) have so far been defined. Influenza virus infection is initiated by the interaction between HA and sialic acid moieties of glycoconjugates on host cells [16].

Several synthetic drugs such as amantadine and rimantadine (M2 ion channel inhibitors) and oseltamivir and zanamivir (NA inhibitors) have been available for decades, but all have side effects and thus somewhat limited usefulness [6, 11]. Therefore, novel substances and approaches are needed to control and prevent this viral disease. Various natural products have distinct anti-influenza virus activities [14]. We have demonstrated that a high-molecular-weight lignin-related fraction extracted from cones of *Pinus parviflora* Siebold et Zucc. suppresses the multiplication of influenza viruses by preventing viral RNA synthesis [9, 15]. We also reported that *Sanicula europaea* L. leaf extract contains an anti-influenza virus substance(s) that selectively inhibits influenza A viruses, but

Published online: 22 November 2012

not influenza B viruses [13]. Studies on the anti-influenza virus activity of natural products have dramatically increased over the past several years [14].

Ginkgo biloba leaf extract (EGb) is a potential phytomedicine with various pharmacologic effects: in particular, anticoagulant, vasodilator, and anti-inflammatory effects [17]. In many countries, EGb and similar products are prescribed as therapeutic agents for cerebral or peripheral vascular inefficiency and for cognitive impairments associated with aging [2, 3]. Unlike other herbal drugs, however, EGb has hardly been tested for its anti-influenza virus activity. In the present study, we examined the inhibitory effect of EGb on influenza viruses.

Materials and methods

Reagents

The powder of *Ginkgo biloba* leaf extract was prepared by Mitsubishi Paper Mills Co., Ltd., Japan. In brief, the dried *Ginkgo biloba* leaves were finely ground and then extracted with water containing alcohol. After removing the residue, the extracts were concentrated under reduced pressure. The concentrate was then filtered and treated with adsorption resin to eliminate the impurities. Finally, the extracts were concentrated under reduced pressure again and then dried to use as powder. The powder of *Ginkgo biloba* leaf extract was dissolved in DMSO at a concentration of 100 mg/ml and stored at −30 °C until use.

As main active ingredients, it is known that the extract contains not only flavonoids such as kaempferol, quercetin and isorhamnetin but also terpene lactones such as bilobalide, ginkgolide A, B, C and J as specific components derived from *Ginkgo biloba* leaves [1, 4, 5].

Cells and viruses

Madin–Darby canine kidney (MDCK) cells were maintained in Eagle's minimum essential medium (MEM) at 37 °C, in a 5 % CO_2 atmosphere, supplemented with 10 % fetal bovine serum, 0.03 % L-glutamine, 100 U/ml penicillin and 100 μg/ml streptomycin.

Influenza A/PR/8/34 (H1N1), A/Udorn/72 (H3N2), and B/Lee/40 viruses were grown at 35.5 °C for 48 h in allantoic sacs of 11-day-old embryonated eggs (Miyake Hatchery), and then the infected allantoic fluid was collected and stored at −80 °C until use.

Neutral red assay

The neutral red assay is based on incorporation of neutral red into lysosomes in living cells. To determine the effect of EGb on cell viability, MDCK cells (3.5×10^4 cells/well) were seeded into 24-well tissue culture plates and kept at 37 °C overnight. After removal of the culture medium, 0.4 ml of MEM containing various concentrations of EGb or DMSO was added to each well of the plates. After incubation for 24 h at 37 °C, 0.2 ml of neutral red solution (0.15 mg/ml) was added to each well. After incubation at 37 °C for 3 h, wells were washed with 0.2 ml of a fixative (1 % formalin and 1 % $CaCl_2$). To extract the dye, 0.2 ml of 1 % acetic acid in 50 % ethanol was added to each well. After incubation at room temperature for 20 min, the amount of neutral red in each well was determined by measuring absorbance at 550 nm using a spectrometer. Results were represented as the cell number that was calculated from the standard curve of cell numbers. Furthermore, to determine the effect of EGb on the cell growth, MDCK cells (2.0×10^4 cells/well) were seeded into 24-well tissue culture plates and kept at 37 °C overnight. After removal of the medium, 0.4 ml of MEM containing 0, 10 and 100 μg/ml of EGb were added to each well. As control groups, DMSO was added to each well at final concentrations of 0.01 or 0.1 %. After incubation at 37 °C for 0, 24, 48 and 72 h, viable cells were determined with the neutral red assay as described above.

Treatment of viruses and cells by EGb

For pre-treatment of viruses by EGb, influenza A/PR/8/34 virus (500 pfu/ml) was mixed with EGb at several concentrations, incubated at room temperature for 10 min, and then subjected to the plaque formation assay. For post-treatment by EGb, MDCK cells infected with influenza viruses were overlaid with 0.8 % agarose containing EGb at several concentrations in the plaque formation assay. To investigate the direct effect of EGb on host cells, MDCK cells were exposed to EGb at several concentrations and incubated at 37 °C for 1 h. After removing the medium containing EGb, MDCK cells were infected with influenza viruses followed by the plaque formation assay.

Plaque formation assay

A confluent monolayer culture of MDCK cells in a 6-well tissue culture plates was washed with serum-free MEM and then infected with 0.5 ml of influenza virus solution [500 pfu/ml = multiplicity of infection (MOI) of 2.5×10^{-4}] in serum-free MEM. After allowing 1 h at 37 °C for virus adsorption, the cells were washed with serum-free MEM and then overlaid with MEM containing 0.8 % agarose, 0.2 % BSA and 1 μg/ml L-1-tosylamide-2-phenylethyl chloromethyl ketone (TPCK)-treated trypsin (Sigma). After incubation at 37 °C for 2–3 days, plaques were visualized by staining cells with 0.5 % amido black.

Results were represented as a ratio of the plaque number formed in the presence of EGb to that in the absence of EGb.

Hemagglutination assay

Influenza A/PR/8/34 virus (2×10^8 pfu/ml) was diluted nine times with phosphate buffered saline (PBS) (−) by twofold dilution each time, while 200 μg/ml of EGb was also diluted ten times with PBS (−) containing 0.2 % DMSO by twofold dilution each time. Fifty microliters of each diluted virus was mixed with 50 μl of each diluted EGb. These mixtures were then maintained at room temperature for 5 min. One hundred microliters of 0.5 % chicken erythrocyte suspension (Nippon Bio-Test Laboratories Inc., Japan) was added to each of these mixtures in 96-well round-bottom plates, and then the plate was incubated at room temperature for 30 min for hemagglutination. Results were represented as a plot where the *x*-axis and *y*-axis indicate concentrations of EGb and HA titer, respectively.

Statistical analysis

All of the data were represented as mean ± standard error of the mean (SEM). Comparisons for all pairs were performed by Student's *t* test. A *p* value >0.05 was considered to be not significant. The calculations of 50 % cytotoxicity concentration (CC_{50}) and inhibitory concentrations with 50 % plaque reduction (IC_{50}) were performed by nonlinear regression using GraphPad Prism's "log (inhibitor) versus response − variable slope" function (GraphPad Prism Version 5.01 for Windows, GraphPad Software Inc.).

Results

Effect of EGb on the viability and growth of MDCK cells

Before examining the anti-influenza virus activity of EGb, we investigated whether EGb affects the viability and growth of MDCK cells, which are routinely used as host cells for influenza viruses. We evaluated the cell viability and growth by counting the number of living cells as a function of time using the neutral red assay as described in "Materials and methods". Cytotoxic effects of EGb were not observed at concentrations of <10 μg/ml (CC_{50} = 180 μg/ml) (Fig. 1a). Neither the growth rate nor the final cell density was affected by the presence of 10 μg/ml of EGb, whereas a marked decrease in the cell growth rate was observed at 100 μg/ml (Fig. 1b). Thus, EGb at a concentration of <10 μg/ml could be considered essentially

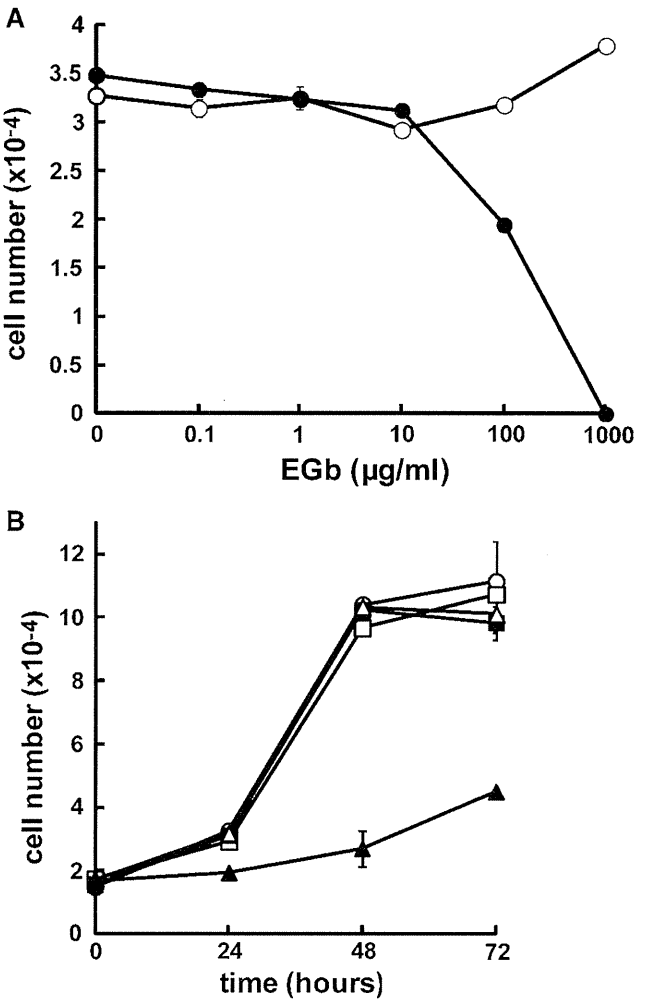

Fig. 1 Effect of EGb on the viability and the growth of MDCK cells. **a** MDCK cells (3.5×10^4) were seeded in 24-well tissue culture plates and incubated at 37 °C in the presence of various concentrations of EGb (*closed circles*) or solvent DMSO alone (*open circles*). After incubation for 24 h, the viable cell number was determined by the neutral red assay. **b** MDCK cells (2×10^4) were seeded in 24-well tissue culture plates and incubated at 37 °C in the absence (*open circles*) or presence of 10 μg/ml (*closed square*) and 100 μg/ml (*closed triangles*) of EGb, and 0.01 % (v/v) and 0.1 % (v/v) of DMSO alone (*open square* and *open triangle*, respectively). After incubation for the indicated periods, the viable cell number was determined by the neutral red assay

nontoxic to MDCK cells. We confirmed that the solvent DMSO had no effect on the viability and growth of MDCK cells in the range of concentrations used in this study (data not shown).

Inhibition of influenza virus infectivity by EGb

To examine whether EGb inhibits multiplication of influenza viruses, plaque assays were carried out as described in "Materials and methods". Cells were infected with influenza A/PR/8/34 virus at 37 °C for 1 h. The cells were

washed extensively with serum-free MEM and then overlaid with 0.8 % agarose in MEM containing EGb at various concentrations. The number of plaques and their sizes in the presence of EGb did not differ from those in the absence of EGb (Fig. 2a), indicating that EGb does not inhibit plaque formation by influenza virus infection. We further examined whether EGb is effective when mixed with viruses before exposure to cells. Influenza viruses were mixed with EGb at various concentrations at room temperature for 10 min and then exposed to MDCK cells. Under these conditions, EGb markedly inhibited viral infectivity in a dose-dependent manner (Fig. 2b). EGb at a concentration of 5 μg/ml almost completely inhibited the plaque-forming activity. These findings suggest that EGb inhibits the initial step of influenza virus infection before the virus enters the cytoplasm. Next, we examined whether the inhibitory effect of EGb against influenza virus was direct or indirect. Plaque assays were performed using MDCK cells treated with EGb at various concentrations for 1 h before infection with the influenza viruses. The number and sizes of the plaques of the tested groups in the presence of EGb did not differ significantly from those of the control group in the absence of EGb (Fig. 3), suggesting that EGb directly interacted with the influenza viruses and markedly reduced their infectivity.

Inhibition of hemagglutination by EGb

Influenza virus infection is initiated by the interaction of hemagglutinin (HA) on the virion with sialic acids on the host cell surface. To understand how EGb prevents virus adsorption to cells, we examined whether EGb competitively inhibits influenza virus-mediated hemagglutination. As shown in Fig. 4, EGb inhibited hemagglutination in a dose-dependent manner, suggesting that EGb interferes with the interaction between HA and sialic acids.

Susceptibility of other influenza virus strains to EGb

Our results suggest that EGb binds to HA and prevents virus adsorption to cells. We further examined whether the inhibitory effect of EGb is dependent on the type of influenza virus. EGb inhibited the infectivity of both influenza A/Udorn/72 (H3N2) and influenza B/Lee/40 viruses as well as of influenza A/PR/8/34 (H1N1) virus in an adsorption inhibition-dependent manner (compare Fig. 5a and b), albeit

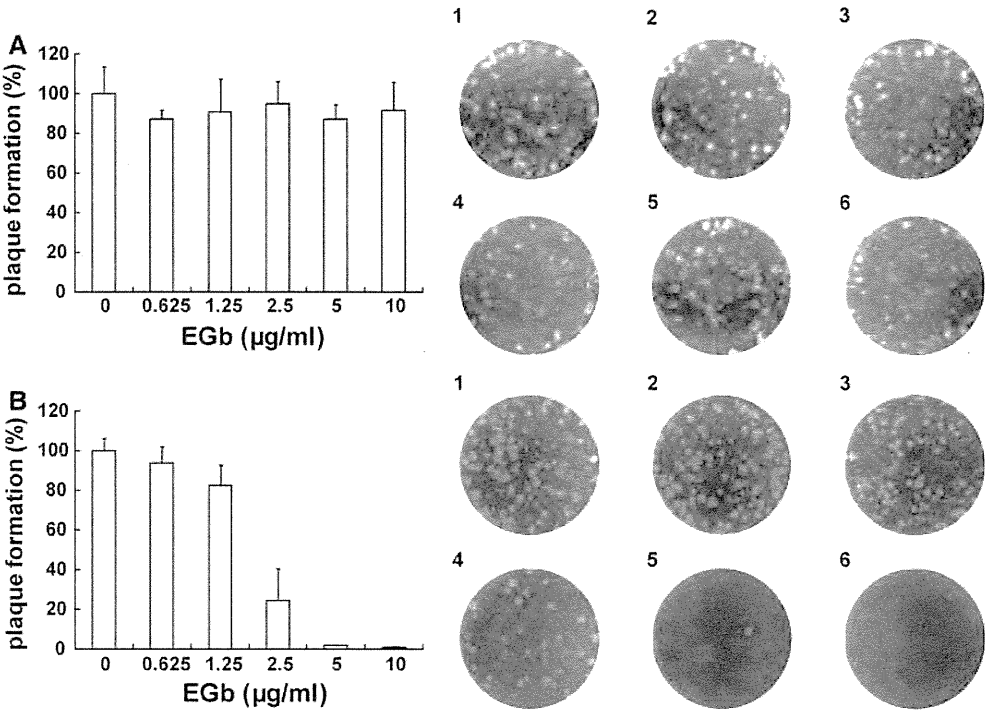

Fig. 2 Effect of EGb on plaque formation. Plaque assays were carried out as described in "Materials and methods". **a** MDCK cells were infected with virus suspension (500 pfu/ml) and then overlaid with the overlay medium containing various concentrations of EGb. The profile of plaques is shown in the *right panels*. *Panels 1*, *2*, *3*, *4*, *5* and *6* represent assays carried out in the presence of 0, 0.625, 1.25, 2.5, 5 and 10 μg/ml of EGb, respectively. **b** Influenza A virus (500 pfu/ml) was incubated with various concentrations of EGb prior to exposure to MDCK cells. The profile of plaques is shown in the *right panels*. *Panels 1*, *2*, *3*, *4*, *5* and *6* represent assays in the presence of 0, 0.625, 1.25, 2.5, 5 and 10 μg/ml of EGb, respectively. Results are represented as the percentage of the plaque number formed in the absence of EGb

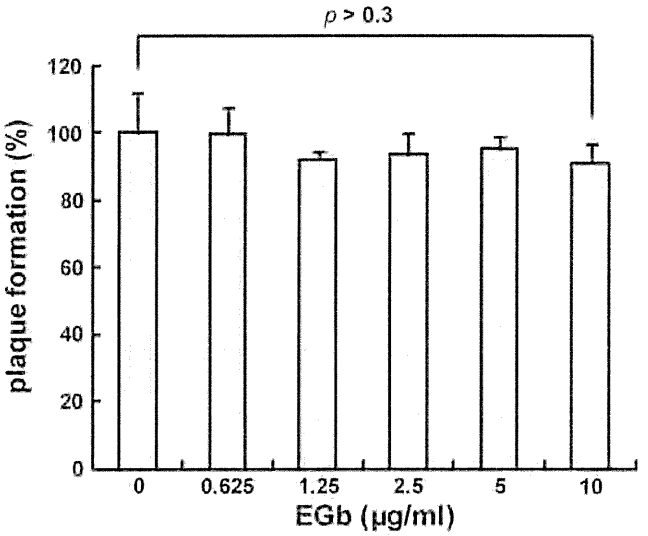

Fig. 3 Effect of pre-treatment of host cells with EGb on influenza virus infection. MDCK cells were exposed to EGb at various concentrations and incubated at 37 °C for 1 h prior to virus infections. After removing EGb, MDCK cells were inoculated with influenza A/PR/8/34 viruses (500 pfu/ml), and plaque formation assays were carried out as described in "Materials and methods". Results are represented as the percentage of the plaque number formed in the absence of EGb. All data are represented as mean ± SD, and the statistical analysis was performed using the *t* test to compare two groups

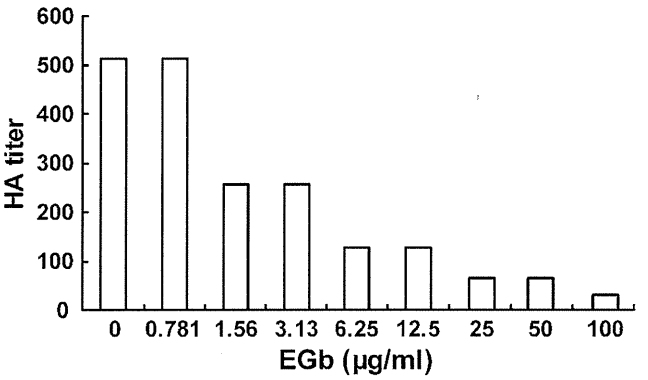

Fig. 4 HA titers of influenza A virus treated with various concentrations of EGb. Influenza A/PR/8/34 virus and EGb were diluted by twofold dilution each time and then mixed. After incubation at room temperature for 5 min, 0.5 % chicken erythrocyte suspension was added to each of these mixtures in a 96-well assay plate, and the plate was incubated at room temperature for 30 min for hemagglutination. Results are represented as a plot where the *x*-axis and *y*-axis indicate concentrations of EGb and HA titer, respectively. The result is representative of three independent experiments

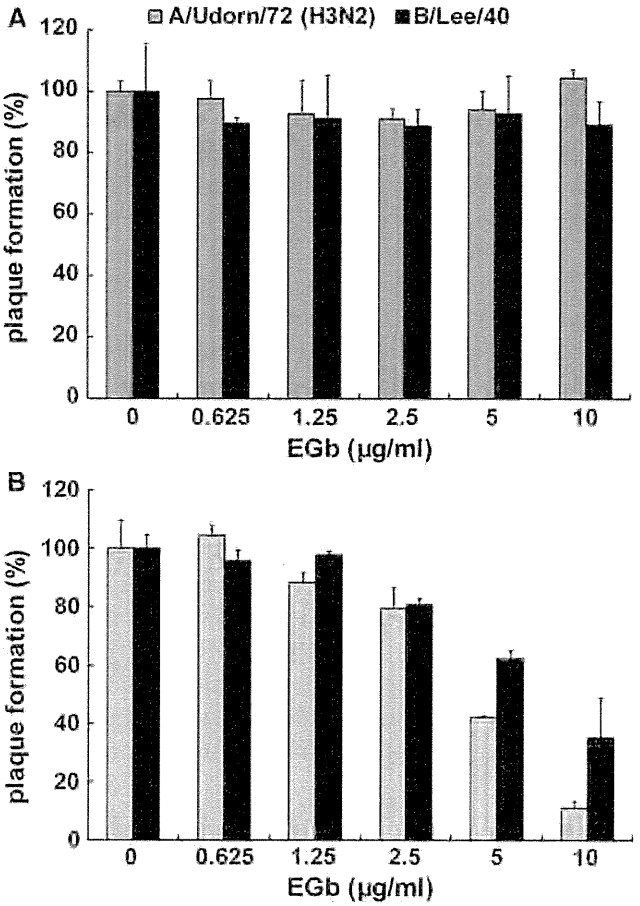

Fig. 5 Effect of EGb on plaque formation by two different subtypes of influenza virus. Plaque assays were carried out as described in "Materials and methods". **a** MDCK cells were infected with 0.5 ml of 500 pfu/ml of influenza A/Udorn/72 (H3N2) and B/Lee/40 viruses and then overlaid with the overlay medium containing various concentrations of EGb. **b** Each influenza virus strain was diluted to 500 pfu/ml and incubated with various concentrations of EGb prior to exposure to MDCK cells. One hour after virus inoculation, MDCK cells were washed with serum-free MEM and subsequently overlaid with the overlay medium without EGb. Results are represented as the percentage of the plaque number formed in the absence of EGb. **a**, **b** Results of A/Udorn/72 (H3N2) and B/Lee/40 are represented by *gray bars* and *black bars*, respectively

with slightly different sensitivities. To confirm the difference in infectivity inhibition, the 50 % inhibitory concentration (IC_{50}) value of EGb was calculated for these three different strains of influenza viruses. Furthermore, the selectivity index (SI) was also calculated as the ratio of CC_{50} to IC_{50} (Table 1). The influenza A/PR/8/34 virus showed most sensitivity to EGb (Table 1). These findings suggest that the antiviral activity of EGb is not dependent on the type of influenza virus.

Discussion

In this study, we revealed the anti-influenza virus activity of *Ginkgo biloba* leaf extract (EGb). EGb acted directly on the influenza viruses and prevented their adsorption to the host cell surface, suggesting that EGb interfered with the interaction between the HA on the influenza virion and sialic acids on the host cell surface, although we could not

Table 1 Selectivity indices of EGb in three different influenza virus strains

Virus strain	IC_{50} (μg/ml)[a]	SI[b]
A/PR/8/34 (H1N1)	1.86	96.8
A/Udorn/72 (H3N2)	4.41	40.8
B/Lee/40	6.79	26.5

[a] IC_{50}: 50 % inhibitory concentration of EGb was calculated from the results of the plaque formation assay performed as shown in Figs. 2b and 5b

[b] SI: selectivity index was evaluated as the ratio of CC_{50} to IC_{50}, i.e., $SI = CC_{50}/IC_{50}$

CC_{50}: 50 % cytotoxic concentration of EGb was calculated from the dose–response curve shown in Fig. 1a and its value (=180 μg/ml) was used for the calculation of each SI

All calculation was performed by using GraphPad Prism software as described in "Materials and methods"

exclude the possibility that EGb had a viricidal activity and directly inactivated the influenza virus.

The active constituents of EGb are standardized around the world; i.e., they contain 24 % flavonol glycosides (quercetin, kaempferol and isorhamnetin) and 6 % terpene lactones (ginkgolides and bilobalide). EGb also contains a class of condensed tannins, which are polymers composed primarily of flavan-3-ols (catechin and epicatechin) with a covalent bond between the individual flavonol units. Nakayama et al. [10] previously reported that two condensed tannins present in teas, (−)-epigallocatechin gallate (EGCG) and theaflavin digallate, bind to the HA of the influenza virus and inhibit its adsorption to MDCK cells. Furthermore, Song et al. [12] showed that catechin derivatives, including EGCG from green tea, inhibit not only the hemagglutination but also the NA activity of the influenza virus. The neuraminidase activity is thought to play a key role in the release of progeny virions from infected cells by cleavage of the sialic acid moieties of host cell receptors and in the prevention of self-aggregation of virions by cleavage of sialic acid still bound to the virus surface. These findings provide important insights into the molecular mechanisms of action of EGb.

Ginkgetin, a biflavone originally isolated from *Ginkgo biloba* leaves, has been found to inhibit the influenza virus sialidase [7]. However, our results showed that EGb prevented adsorption in the initial step of influenza virus infection. Therefore, in our study, a substance(s) in EGb other than ginkgetin may have been effective against influenza virus infection.

EGb was effective against the three different types of influenza viruses tested here, viz., the influenza A/PR/8/34 (H1N1), A/Udorn/72 (H3N2), and B/Lee/40 viruses, although the sensitivity towards EGb was slightly different among the three viruses. This finding suggests that EGb may be a potential wide-range inhibitor against influenza virus infection.

When plaque assays were performed with overlay medium containing EGb, neither the number of plaques nor their sizes were affected (Fig. 2a). Since our results suggest that EGb acts directly on the influenza virus and prevents the initial step in viral infection, we expected that the infectivity of the progenitor virions would be decreased owing to interaction with EGb present in the overlay medium and, consequently, that the size of individual plaques would be reduced in the plaque assay. This discrepancy between the predicted and the experimental results may be explained by our recent findings: we disclosed a novel transmission mode for influenza viruses, the so-called cell-to-cell transmission mode [8]. Influenza viruses have generally been believed to be capable of spreading via *cell-free* virions released from infected cells depending on the activity of NA. However, in cell-to-cell transmission, progeny virions are retained on the infected cell surface even after budding and transmitted from infected cells to adjacent uninfected cells without being released into the outer environment. The cell-to-cell transmission of the influenza virus is dependent on functional HA but independent of NA activity. The present study may demonstrate that EGb cannot inhibit the cell-to-cell transmission of influenza viruses but is highly effective in decreasing the infectivity of *cell-free* virions. This suggestion is in line with the findings of a previous study in which higher concentrations of anti-HA antibody were needed for inhibition of infection through cell-to-cell transmission than for that through *cell-free* viruses [8].

The plaque assay using drug-containing agarose gels is one of the most reliable methods for detecting anti-influenza virus activity and is frequently used as a screening method. However, our findings raise concerns that a particular anti-influenza virus activity, such as the inhibitory effect found here in EGb, may have been largely overlooked in past studies.

In conclusion, we have shown that EGb interacts directly with influenza viruses and markedly reduces the infectivity of the viruses by preventing their adsorption to host cells. Furthermore, the inhibitory effect of EGb seemed not to be restricted to a certain subtype of influenza virus. Taken together, these findings indicate the usefulness of EGb as an antiviral agent for influenza, although further studies are necessary to confirm its anti-influenza virus activity in vivo.

In addition to the finding of the anti-influenza virus activity of EGb, we demonstrated an interesting and important insight(s) into the screening system for anti-influenza virus activity. As was the case for the anti-influenza virus activity of EGb found in this study, some candidates for antiviral agents may have been overlooked